Figure 1. Structures of T140 and its downsized peptide FC131. Circled residues are the indispensable residues of T140 for the expression of strong CXCR4-antagonistic activity. Nal = L-3-(2-naphthyl)alanine, Cit = L-citrulline.

peptide with a disulfide bridge, and we identified four critical residues: Arg^2, Nal^3, Tyr^5, and Arg^{14} (Figure 1).[28–30] Molecular-size reduction of T140 based on the structural requirement led to the discovery of FC131, which has a cyclic pentapeptide template,[31–37] with CXCR4-antagonistic and anti-HIV activity comparable to those of T140.[16] We wish to investigate contributions of each amide bond in FC131 to the biological activity in order to develop pseudopeptides, in which the peptide character is reduced to obtain more druglike structures. For this purpose, EADIs and reduced amide-type dipeptide isosteres (RADIs) of Arg-Nal and Nal-Gly are required, because the amide bonds between Arg^2 and Nal^3 and between Nal^3 and Cys^4 were found to be cleaved by treatment of T140 analogues with rat liver homogenates.[38,39] Thus, (L-Arg-L/D-Nal)-type EADIs were synthesized in the study described here, and a (Nal-Gly)-type EADI was also synthesized by another method using the samarium diiodide (SmI$_2$)-induced reduction of a γ-acetoxy-α,β-enoate.[40,41] RADIs of Arg-Nal and Nal-Gly were prepared by a standard method of reductive amination. Then, several FC131 analogues, in which the above isosteres were introduced, were synthesized to identify the biological importance of these amide bonds.

Results and Discussion

Synthesis of (L-Arg-L/D-Nal)-Type EADIs. (L-Arg-L/D-Nal)-type EADIs were synthesized via the same key intermediate N-2-nitrobenzenesulfonyl (Ns)-γ,δ-cis-γ,δ-epimino (E)-α,β-enoate, **9**, as synthetic model compounds for the investigation of the feasibility of α-alkylation using organozinc—copper reagents as well as precursor dipeptide isosteres used for the synthesis of partial nonpeptide analogues of FC131 (Scheme 2). Boc-Arg(Mts)-OMe (Mts = 2,4,6-trimethylbenzenesulfonyl) **5** was treated successively with diisobutylaluminum hydride (DIBAL-H) and vinylmagnesium chloride (CH$_2$=CHMgCl) to give exclusively the *threo*-amino alcohol **6** (a separable mixture of allyl alcohol **6**/*erythro*-isomer of **6** = 12:1). N^α-Ns protection[42,43] after the cleavage of the N^α-Boc group of **6** with HCl/dioxane followed by successive treatments consisting of the Mitsunobu reaction,[44] ozonolysis, and the modified Horner—Wadsworth—Emmons olefination[45] afforded *cis*-(E)-enoate **9**. *Anti*-S$_N$2$'$ reaction of **9** with an organozinc—copper reagent,[11–15] 2-naphthylmethylCu(CN)-ZnBr·2LiCl, afforded an L,L-type EADI **10**, in which a $(2R)$-2-naphthylmethyl side chain was incorporated at the α-position, stereoselectively in 83% yield (diastereoselection > 99:1 from NMR analysis). N^α-Fmoc substitution for the N^α-Ns group of **10** followed by selective deprotection of the benzyl ester using thioanisole/TFA afforded a desired EADI, Fmoc-L-Arg(Mts)-ψ-

[(E)-CH=CH]-L-Nal-OH, **12**. Alternatively, exposure of **9** to MSA/CHCl$_3$ afforded exclusively δ-aminated γ-mesyloxy-α,β-enoate **13** by regio- and stereoselective S$_N$2 ring-opening reaction at the γ-carbon of **9**. Mesylate **13** was successively treated by an organozinc—copper reagent, 2-naphthylmethylCu(CN)ZnBr·BF$_3$, to afford an L,D-type EADI **14**, in which a $(2S)$-2-naphthylmethyl side chain was incorporated at the α-position, stereoselectively via an *anti*-S$_N$2$'$mechanism in 67% yield (diastereoselection > 99:1 from NMR analysis). **14** was similarly converted into another desired EADI, Fmoc-L-Arg(Mts)-ψ[(E)-CH=CH]-D-Nal-OH, **16**. As such, α-alkylation of both a *cis*-(E)-enoate and its ring-opened product using organozinc—copper reagents was successfully performed in the synthesis of (L-Arg-L/D-Nal)-type EADIs. An N-Ns group could be used in this synthetic scheme as an orthogonal N-protecting (activating) group instead of an N-Mts or N-Ts group. Relative configurations of the allyl alcohols (**6** and its erythro isomer) were determined by comparative nuclear Overhauser effect (NOE) measurements of these oxazolidinone derivatives **17** and **18** (Scheme 2).[2] The (E)-geometry of the double bond in the synthesized EADIs was assigned based on the coupling constant of the two olefinic protons on ^{1}H NMR analysis.

Synthesis of (L-Nal-Gly)-Type EADI. An (L-Nal-Gly)-type EADI was synthesized as shown in Scheme 3. Boc-L-Nal-OMe **19** was treated sequentially with DIBAL-H and CH$_2$=CHMgCl to give a diastereomixture of allyl alcohol **20**. Acetylation of **20** followed by ozonolysis and the modified Horner—Wadsworth—Emmons olefination afforded a γ-acetoxy-α,β-unsaturated ester **22**. Acetate **22** was reduced with SmI$_2$-^{t}BuOH to yield an (L-Nal-Gly)-type EADI **23** in 95% yield,[40,41] followed by deprotection of the N^α-Boc group and *tert*-butyl ester with TFA and reprotection with an N^α-Fmoc group to afford the desired EADI, Fmoc-L-Nal-ψ[(E)-CH=CH]-Gly-OH, **24**.

Synthesis of RADIs of Arg-Nal and Nal-Gly. (L-Arg-L-Nal)- and (L-Nal-Gly)-type RADIs were prepared for comparative studies. As shown in Scheme 4, Arg- and Nal-derived Weinreb amides **25** and **29** were treated with DIBAL-H to afford the corresponding aldehyde derivatives. Subsequently, reductive amination of the aldehydes was performed by treatments with carboxy-protected amino acids in the presence of acetic acid and sodium triacetoxy borohydride [NaBH(OAc)$_3$] to afford secondary amines **26** and **30**, respectively.[46] Protection of the *sec*-amino groups with Cbz groups followed by deprotection of the N^α-Boc group and *tert*-butyl ester with TFA and reprotection with an N^α-Fmoc group afforded the desired RADIs, Fmoc-L-Arg(Mts)-ψ-[CH$_2$-N(Cbz)]-L-Nal-OH, **28**, and Fmoc-L-Nal-ψ[CH$_2$-N(Cbz)]-Gly-OH, **32**, respectively.

Synthesis of Cyclic Pseudopeptides. The protected peptide chains were constructed on a hydrazino resin **34** by Fmoc-based solid-phase synthesis using ^{t}Bu and 2,2,4,6,7-pentamethyldihydrobenzofuran-5-sulfonyl (Pbf) groups for side-chain protection of D-Tyr and Arg, respectively (Scheme 5). N^α-Fmoc-protected dipeptide isosteres, EADIs **12**, **16**, and **24** and RADIs **28** and **32**, were similarly condensed. In the synthesis of cyclic pseudopeptides, two steps of deprotection/cleavage were adopted to prevent guanidino groups of Arg from

Scheme 2[a]
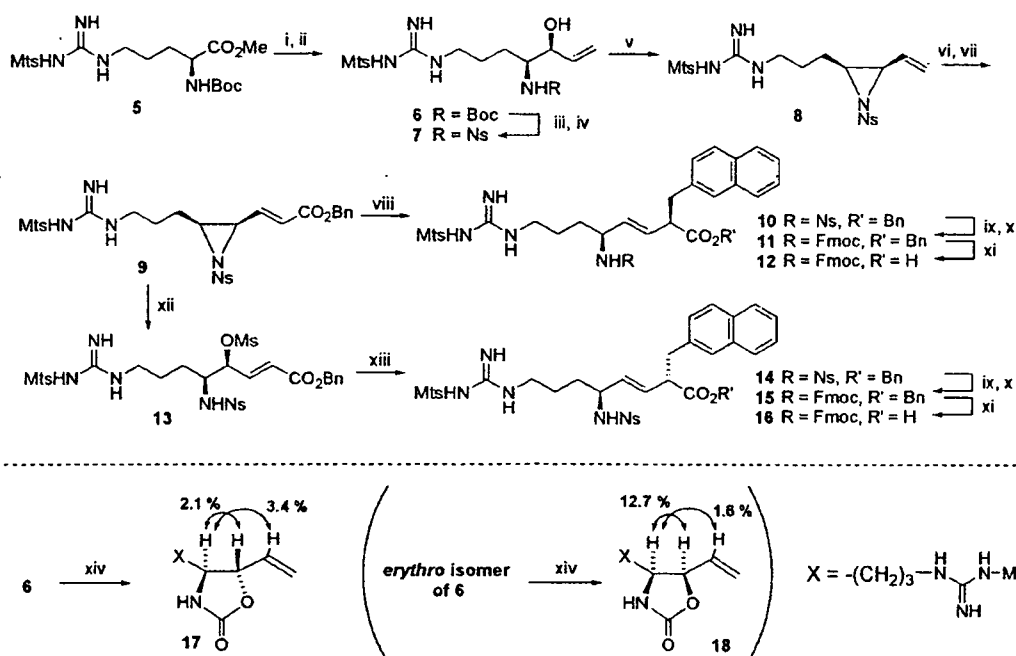
[a] Reagents: (i) DIBAL-H; (ii) CH2=CHMgCl; (iii) HCl, anisole; (iv) Ns-Cl, pyridine; (v) Ph3P, DEAD; (vi) O3, then Me2S; (vii) (EtO)2P(O)CH2CO2Bn, LiCl, DIPEA; (viii) 2-naphthylmethylCu(CN)ZnBr·2LiCl; (ix) PhSH, K2CO3; (x) Fmoc-OSu, Et3N; (xi) thioanisole, TFA; (xii) MsOH; (xiii) 2-naphthylmethylCu(CN)ZnBr·BF3; (xiv) NaH.

Scheme 3[a]
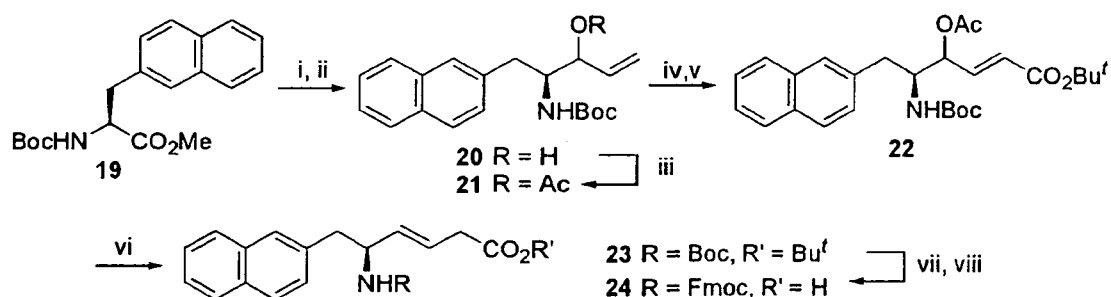
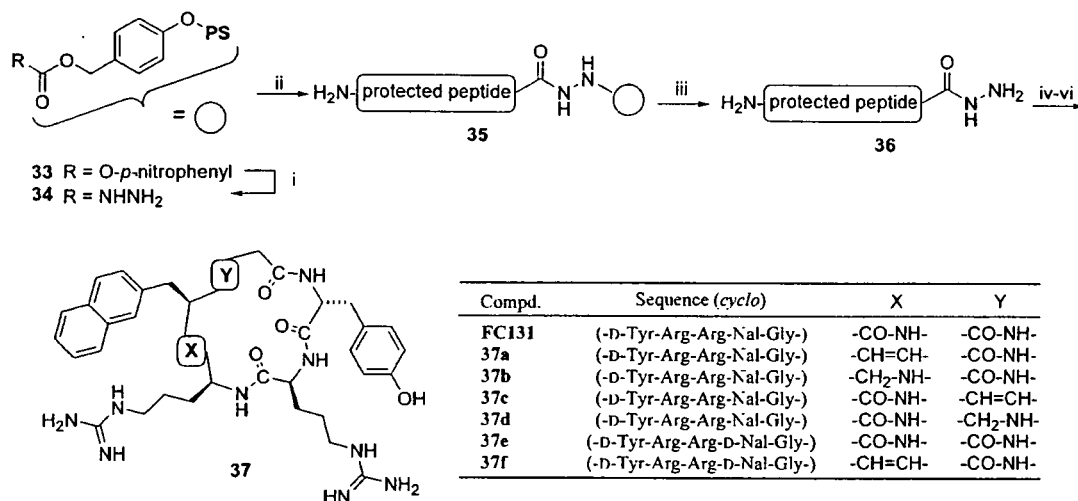[a] Reagents: (i) DIBAL-H; (ii) CH2=CHMgCl; (iii) Ac2O, DMAP, pyridine; (iv) O3, then Me2S; (v) (EtO)2P(O)CH2CO2[t]Bu, LiCl, DIPEA; (vi) SmI2, [t]BuOH; (vii) anisole, TFA; (viii) Fmoc-OSu, Et3N.

Scheme 4[a]
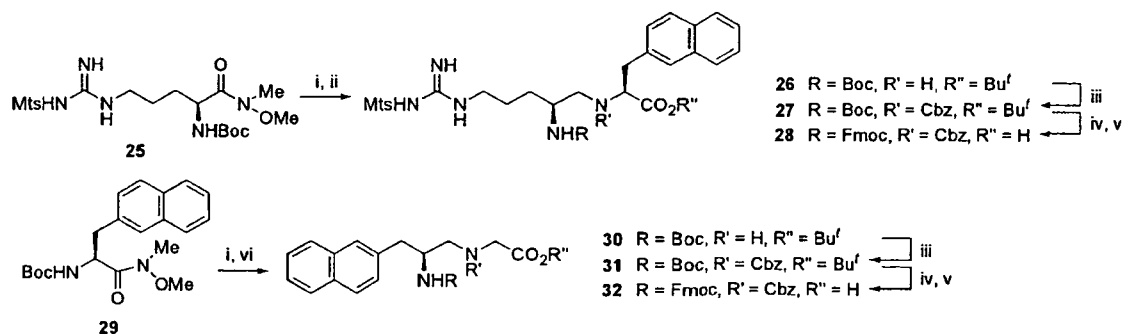
[a] Reagents: (i) DIBAL-H; (ii) H-Nal-O[t]Bu, AcOH, NaBH(OAc)3; (iii) Cbz-Cl, Et3N; (iv) anisole, TFA; (v) Fmoc-OSu, Et3N; (vi) H-Gly-O[t]Bu, AcOH, NaBH(OAc)3.

participating in cyclizing reaction as follows. After construction of peptide chains, pseudopeptide hydrazides **36** were obtained by cleavage from the resin

35 using 10% TFA/CHCl3 without cleavage of Pbf, Mts, and Cbz groups (first deprotection). Cyclization of linear pseudopeptides by the azide procedure[47] in highly

Scheme 5[a]

33 R = O-*p*-nitrophenyl
34 R = NHNH₂

Compd.	Sequence (cyclo)	X	Y
FC131	(-D-Tyr-Arg-Arg-Nal-Gly-)	-CO-NH-	-CO-NH-
37a	(-D-Tyr-Arg-Arg-Nal-Gly-)	-CH=CH-	-CO-NH-
37b	(-D-Tyr-Arg-Arg-Nal-Gly-)	-CH₂-NH-	-CO-NH-
37c	(-D-Tyr-Arg-Arg-Nal-Gly-)	-CO-NH-	-CH=CH-
37d	(-D-Tyr-Arg-Arg-Nal-Gly-)	-CO-NH-	-CH₂-NH-
37e	(-D-Tyr-Arg-Arg-D-Nal-Gly-)	-CO-NH-	-CO-NH-
37f	(-D-Tyr-Arg-Arg-D-Nal-Gly-)	-CH=CH-	-CO-NH-

[a] Reagents: (i) NH₂NH₂·H₂O; (ii) Fmoc-based SPPS; (iii) TFA; (iv) HCl, isoamyl nitrite; (v) DIPEA; (vi) 1 M TMSBr−thioanisole/TFA, *m*-cresol, 1,2-ethanedithiol.

**Table 1.** Activity and Cytotoxicity of the Synthetic Compounds

compound (no.)	CC₅₀[a] (μM)	EC₅₀[b] (μM)	IC₅₀[c] (μM)
FC131	> 100	0.073	0.0045 ± 0.0018
37a	> 100	2.4	31–100[d]
37b	> 100	> 100	> 100
37c	> 100	2.4	0.18 ± 0.10
37d	> 100	0.98	0.032 ± 0.011
37e	> 100	1.9	0.19 ± 0.071
37f	> 100	9.1	21
T140	> 10	0.035	0.0039 ± 0.0004
AZT	57	0.018	

[a] CC₅₀ values are based on the reduction of the viability of mock-infected MT-4 cells. Because the cytotoxicity of T140 was previously evaluated as CC₅₀ > 40 μM, further estimation at high concentrations was omitted in this study. [b] EC₅₀ values are based on the inhibition of HIV-induced cytopathogenicity in MT-4 cells. [c] IC₅₀ values are based on the inhibition of [¹²⁵I]-SDF-1-binding to CXCR4 transfectants of CHO cells. All data are the mean values for at least three independent experiments. [d] 37a showed significant antagonistic activity in 100 μM but hardly showed activity in 31 μM.

diluted dimethylformamide (DMF) solution followed by deprotection of Pbf, Mts, and Cbz groups with 1 M TMSBr−thioanisole/TFA (second deprotection) gave the desired cyclic pseudopeptides **37**.

Biological and Conformational Evaluation of Synthetic Cyclic Pseudopeptides. Anti-HIV activity based on the inhibition of HIV-1-induced cytopathogenicity in MT-4 cells was evaluated using the 3-(4,5-dimethylthiazol-2-yl)-2,5-diphenyltetrazolium bromide (MTT) method.[46] CXCR4-antagonistic activity was evaluated by the inhibition of [¹²⁵I]-SDF-1-binding to CXCR4 transfectants of CHO cells.[49] **37a**, an (L-Arg-L-Nal)-type EADI containing FC131 analogue, showed moderate anti-HIV activity (EC₅₀ = 2.4 μM) and CXCR4-antagonistic activity (100 μM > IC₅₀ > 31 μM). Introduction of an EADI into the Arg-Nal sequence caused a remarkable decrease in anti-HIV activity (33-fold lower activity). NMR and simulated annealing molecular dynamics (SA-MD) analysis of **37a** showed a pseudopeptide backbone structure with a nearly symmetrical pentagonal

shape similar to that of FC131,[16] excluding the difference between the orientation of two protons in the (*E*)-alkene unit of **37a** and that of the carbonyl oxygen/ amino proton in the Arg-Nal amide bond of FC131 (Figure 2a).[50] Substitution for the amide bond with the EADI caused an inversion of the olefinic plane (180° rotation of pseudo ψ and φ bonds), possibly due to dissolution of the 1,3-pseudo-allylic strain between the carbonyl group of Arg and the side chain of Nal. Introduction of an EADI into the Arg-D-Nal sequence of **37e** (an FC131 epimer, EC₅₀ = 1.9 μM, IC₅₀ = 190 nM) also caused a significant but moderate decrease in anti-HIV activity (the activity of **37f** is 5-fold lower than that of **37e**). The amide bonds of the Arg-L/D-Nal sequences were necessary for high potency. These results suggested that either a deletion of the hydrogen bond interaction with CXCR4 by the insertion of an EADI or an increase in hydrophobicity might be unsuitable. **37b**, an (L-Arg-L-Nal)-type RADI-containing FC131 analogue, did not show anti-HIV or CXCR4-antagonistic activity up to the concentration of 100 μM, suggesting that the planar nature of the amide bond is critical to maintain the pentagonal global conformation for high anti-HIV activity and that the replacement of the amide bond with RADI causes a conformational change of FC131. **37c**, an (L-Nal-Gly)-type EADI-containing FC131 analogue, showed almost the same anti-HIV activity (EC₅₀ = 2.4 μM) as **37a** containing an (L-Arg-L-Nal)-type EADI. NMR and SA-MD analysis of **37c** showed a similar backbone structure with FC131 (Figure 2b).[50] The Nal-Gly amide bond was replaced by the EADI without an inversion of the olefinic plane. **37d**, an (L-Nal-Gly)-type RADI-containing FC131 analogue, exhibited relatively higher anti-HIV and CXCR4-antagonistic activities (EC₅₀ = 0.98 μM, IC₅₀ = 32 nM) than **37c** (IC₅₀ = 180 nM), although these activities were weaker than those of FC131. These results also indicated an importance of the amide bond of the Nal-Gly sequence, as in the case of the Arg-Nal amide bond.

(A) **(B)**
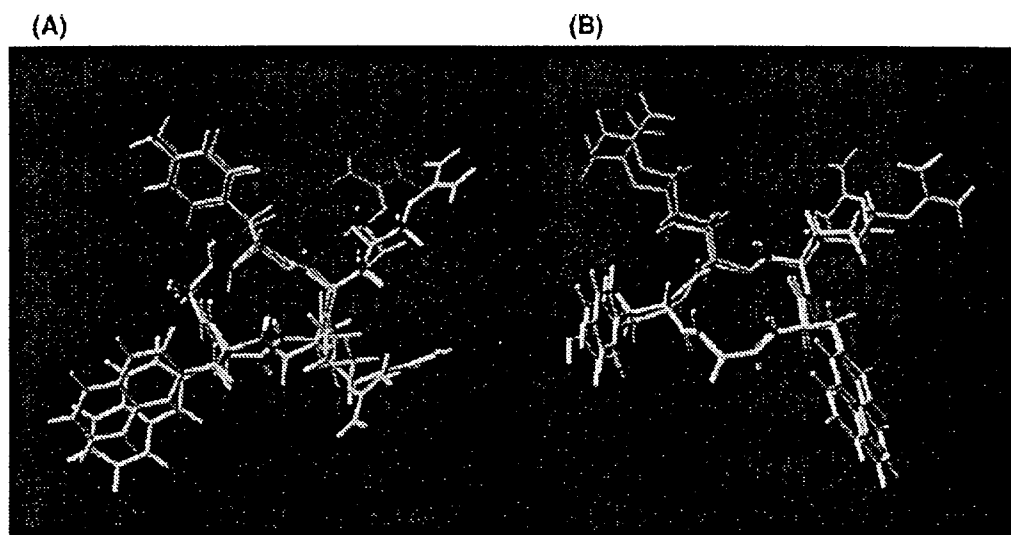
Figure 2. Superimpositions of low-energy structures of FC131 and **37a** (A) or **37c** (B). The FC131 structure is depicted in green, and the **37a** or **37c** structure is depicted in purple.

Conclusion

A set of (L-Arg-L/D-Nal)-type EADIs were synthesized from a single substrate of γ,δ-*cis*-γ,δ-epimino (E)-α,β-enoate by combination of MSA-mediated aziridinyl ring-opening reactions and *anti*-S_N2' reactions with organozinc—copper reagents that were prepared from 2-naphthylmethylZnBr and CuCN. Organozinc—copper-mediated α-alkylation reactions are thought to be useful for construction of several side chains at the α-position of EADIs, as organocopper-mediated α-alkylation reactions that have been generally used. Next, EADIs and RADIs of Arg-Nal and Nal-Gly, including the above EADIs, were synthesized and inserted into cyclic pentapeptides, FC131 analogues, to disclose biological importance of each amide bond. The present results will be useful for the development of nonpeptide CXCR4 antagonists derived from FC131. It is also noteworthy that EADI units were introduced into cyclic pentapeptides without any significant conformational changes in the pentagonal backbone structures, except for those of substituted (E)-alkene units, suggesting that the planar nature of (E)-alkene units caused the conformational maintenance of the backbones excluding the olefinic moiety. SA–MD analysis showed that the parent peptide (FC131) and the EADI-introduced pseudopeptides (**37a** and **37c**) have nearly equal distances between any two β-carbons in all of the side chains. It suggests that these compounds maintain similar dispositions of pharmacophores and that the biological differences between these compounds are derived from the (E)-alkene/amide bond units. As such, EADIs become useful tools for investigation of biological contributions of amide bonds.

Experimental Section

General. Melting points are uncorrected. ^{1}H NMR spectra were recorded using a JEOL EX-270, a JEOL AL-400, or a Bruker AM 600 spectrometer at 270, 400, or 600 MHz ^{1}H frequency in CDCl$_3$, respectively. Chemical shifts are reported in parts per million downfield from internal tetramethylsilane. Nominal (LRMS) and exact mass (HRMS) spectra were recorded on a JEOL JMS-01SG-2 or JMS-HX/HX 110A mass spectrometer. Ion-spray (IS)-mass spectrum was obtained with a Sciex API III/E triple quadrupole mass spectrometer (Toronto,

Canada). Optical rotations were measured in CHCl$_3$ or H$_2$O with a JASCO DIP-360 digital polarimeter (Tokyo, Japan) or a Horiba high-sensitive polarimeter SEPA-200 (Kyoto, Japan). For flash column chromatography, silica gel 60 H (silica gel for thin-layer chromatography, Merck) and Wakogel C-200 (silica gel for column chromatography) were employed. HPLC solvents were H$_2$O and MeCN, both containing 0.1% (v/v) TFA. For analytical HPLC, a Cosmosil 5C18-AR column (4.6 mm × 250 mm, Nacalai Tesque Inc., Kyoto, Japan) was eluted with a linear gradient of MeCN at a flow rate of 1 mL/min on a Waters model 600 (Nihon Millipore, Ltd., Tokyo, Japan). Preparative HPLC was performed on a Waters Delta Prep 4000 equipped with a Cosmosil 5C18-AR column (20 mm × 250 mm, Nacalai Tesque Inc.) using an isocratic mode of MeCN at a flow rate of 15 mL/min.

Boc-Arg(Mts)-OMe, 5. To a stirred solution of Boc-Arg-(Mts)-OH (10.0 g, 21.9 mmol) in DMF (50 mL) at 4 °C were added potassium bicarbonate (4.39 g, 43.8 mmol) and methyl iodide (2.73 mL, 43.8 mmol), and the mixture was stirred at room temperature for 10 h. The reaction mixture was concentrated under reduced pressure. The residue was extracted with EtOAc, and the extract was washed successively with saturated citric acid, brine, saturated aqueous NaHCO$_3$, and brine and dried over MgSO$_4$. Concentration under reduced pressure gave 10.4 g (21.8 mmol, 100%) of methyl ester 5 as a yellow oil.

[α]^{22}$_D$ −4.25 (c 0.47, CHCl$_3$). ^{1}H NMR (270 MHz, CDCl$_3$) δ: 1.42 (9H, s, *tert*-Bu), 1.61 (2H, br m, CH$_2$), 1.78 (2H, br m, CH$_2$), 2.59 (3H, s, Ar-*p*-Me), 2.66 (6H, s, Ar-*o*-Me), 3.22 (2H, br m, CH$_2$), 3.73 (3H, s, OMe), 4.21−4.28 (1H, m, CH), 5.23 (1H, d, J = 8.2 Hz, NH), 6.14 (3H, br, guanidino), 6.89 (2H, s, ArH). m/z (FAB-LRMS): 471 (MH$^+$), 415, 371, 289 (base peak), 119. Found (FAB-HRMS): 471.2268. Calcd for C$_{21}$H$_{35}$O$_6$N$_5$S (MH$^+$): 471.2277.

*N-tert-*Butoxy-[2(S)-hydroxy-1(S)-[3-[[imino[[(2,4,6-tri-methylphenyl)sulfonyl]amino]methyl]amino]propyl]but-3-enyl]formamide, 6. To a stirred solution of Boc-Arg(Mts)-OMe, 5 (5.0 g, 10.6 mmol), in toluene/CH$_2$Cl$_2$ (1:1 (v/v) 100 mL) was added dropwise a solution of DIBAL-H in toluene (1.0 M, 32 mL, 32 mmol) at −50 °C under argon, and the mixture was stirred at −78 °C for 2 h. To the solution, was added dropwise a vinyl Grignard (CH$_2$=CHMgCl) reagent in THF (13 mL, 32 mmol) at −78 °C, and the mixture was stirred for 6 h with a gradual warming to 0 °C. The reaction was quenched with saturated aqueous citric acid at −78 °C, and organic solvents were concentrated under reduced pressure. The residue was extracted with EtOAc, and the extract was washed successively with saturated aqueous citric acid, satu-

rated aqueous NaHCO₃, and brine and dried over MgSO₄. Concentration under reduced pressure followed by flash column chromatography over silica gel with EtOAc/*n*-hexane (2:1) gave a *threo*-allyl alcohol **6** and an *erythro*-allyl alcohol (2*R* isomer of **6**) (12:1), in order of elution (6, 1.5 g, 30% yield from **5**).

Compound **6**: colorless oil. [α]²²_D −15.74 (*c* 0.63, CHCl₃). ¹H NMR (270 MHz, CDCl₃) δ: 1.40 (9H, s, *tert*-Bu), 1.57 (2H, br m; 2-CH₂), 1.70 (2H, br m, 1-CH₂), 2.26 (3H, s, Ar-*p*-Me), 2.66 (6H, s, Ar-*o*-Me), 3.24 (2H, br m, 3-CH₂), 3.55 (1H, br, 1-H), 4.08 (1H, br, 2-H), 4.97 (1H, d, *J* = 9.7 Hz, NH), 5.18 (1H, d, *J* = 10.5 Hz, C*H*H=), 5.28 (1H, d, *J* = 17.3 Hz, CH*H*=), 5.77−5.89 (1H, m, CH=), 6.20 (3H, br, guanidino), 6.89 (2H, s, ArH). *m/z* (ISMS): 469.5 (MH⁺). Found (FAB-HRMS): 469.2490. Calcd for C₂₂H₃₇O₅N₄S (MH⁺): 469.2485.

Compound 2*R* isomer of **6**: colorless oil. [α]²¹_D −4.57 (*c* 2.84, CHCl₃). ¹H NMR (270 MHz, CDCl₃) δ: 1.41 (9H, s, *tert*-Bu), 1.48 (2H, br m, 2-CH₂), 1.64 (2H, br m, 1-CH₂), 2.30 (3H, s, Ar-*p*-Me), 2.63 (6H, s, Ar-*o*-Me), 3.15 (2H, br m, 3-CH₂), 3.63 (1H, br, 1-H), 4.18 (1H, br, 2-H), 5.12 (1H, br, NH), 5.24 (1H, d, *J* = 10.5 Hz, C*H*H=), 5.32 (1H, d, *J* = 17.0 Hz, C*H*H=), 5.74−5.85 (1H, m, CH=), 6.32 (3H, br, guanidino), 6.95 (2H, s, ArH). *m/z* (ISMS): 469.5 (MH⁺).

[2(*S*)-Hydroxy-1(*S*)-[3-[[imino[[(2,4,6-trimethylphenyl)-sulfonyl]amino]methyl]amino]propyl]but-3-enyl][(2-nitro-phenyl)sulfonyl]amine, 7. To a mixture of allyl alcohol **6** (4.2 g, 9.0 mmol) and anisole (0.97 mL, 9.0 mmol) at 0 °C was added 4 M HCl/dioxane (100 mL), and the mixture was stirred at room temperature for 2 h. The mixture was concentrated under reduced pressure. To a stirred solution of the residue in CHCl₃ (20 mL) at 0 °C were added 2-nitrobenzenesulfonyl chloride (2.38 g, 10.8 mmol), triethylamine (Et₃N) (5 mL), and pyridine (20 mL), and the mixture was allowed to warm to room temperature, stirred at this temperature for 12 h, and extracted with CHCl₃. The extract was washed with saturated aqueous citric acid, saturated aqueous NaHCO₃, and brine and dried over MgSO₄. Concentration under reduced pressure followed by chromatography over silica gel with CHCl₃/MeOH (18:1) gave 3.2 g (5.8 mmol, 65% from **6**) of **7** as a yellow oil.

[α]²³_D −57.79 (*c* 1.83, CHCl₃). ¹H NMR (270 MHz, CDCl₃) δ: 1.61 (4H, br m, 1, 2-CH₂), 2.27 (3H, s, Ar-*p*-Me), 2.64 (6H, s, Ar-*o*-Me), 3.15 (2H, br m, 3-CH₂), 3.50 (1H, br, 1-H), 3.72−3.78 (1H, m, 2-H), 4.72 (1H, d, *J* = 10.5 Hz, C*H*H=), 5.07 (1H, d, *J* = 17.0 Hz, CH*H*=), 5.42−5.48 (1H, m, CH=), 5.90 (1H, d, *J* = 8.1 Hz, NH), 6.26 (3H, br, guanidino), 6.90 (2H, s, ArH), 7.65−7.69 (2H, m, ArH), 7.78−7.82 (1H, m, ArH), 8.04−8.08 (1H, m, ArH). *m/z* (ISMS): 554.5 (MH⁺). Found (FAB-HRMS): 554.1735. Calcd for C₂₃H₃₂O₇N₅S₂ (MH⁺): 554.1743.

3(*S*)-[3-[[Imino[[(2,4,6-trimethylphenyl)sulfonyl]ami-no]methyl]amino]propyl]-1-[(2-nitrophenyl)sulfonyl]-2(*R*)-vinylaziridine, 8. To a stirred solution of allyl alcohol **7** (3.1 g, 5.6 mmol) in dry THF (30 mL) at 0 °C were added triphenylphosphine (1.6 g, 6.2 mmol) and diethyl azodicar-bonate (2.4 mL of a 40% solution in toluene, 6.2 mmol), and the reaction mixture was stirred at this temperature for 30 min. The mixture was concentrated under reduced pressure and purified by chromatography over silica gel with EtOAc/*n*-hexane (2:1) to give 2.8 g (5.2 mmol, 93% yield from **7**) of aziridine **8** as a yellow oil.

[α]²³_D −10.45 (*c* 2.20, CHCl₃). ¹H NMR (270 MHz, CDCl₃) δ: 1.48 (4H, br m, 1, 2-CH₂), 2.26 (3H, s, Ar-*p*-Me), 2.65 (6H, s, Ar-*o*-Me), 3.02 (1H, br, 2-H), 3.15 (2H, br m, 3-CH₂), 3.46 (1H, br, 3-H), 5.29 (1H, d, *J* = 9.7 Hz, C*H*H=), 5.42 (1H, d, *J* = 17.0 Hz, CH*H*=), 5.45−5.53 (1H, m, CH=), 6.41 (3H, br, guanidino), 6.88 (2H, s, ArH), 7.45−7.50 (2H, m, ArH), 7.54−7.75 (2H, m, ArH). *m/z* (ISMS): 536.5 (MH⁺). Found (FAB-HRMS): 536.1630. Calcd for C₂₃H₃₀O₆N₅S₂ (MH⁺): 536.1638.

Phenylmethyl 3-3(*S*)-[3-[[Imino[[(2, 4, 6-trimethylphe-nyl)sulfonyl]amino]methyl]amino]propyl]-2(*R*)-[(2-nitro-phenyl)sulfonyl-2-aziridinyl]prop-2-enoate, 9. To a solu-tion of aziridine **8** (1.2 g, 2.2 mmol) in CH₂Cl₂ (30 mL) was bubbled O₃ gas at −78 °C until a blue color persisted. To the above solution was added Me₂S (1.7 mL, 22 mmol), and the mixture was stirred for 30 min and then dried over MgSO₄.

Concentration under reduced pressure gave an oily residue of a crude aldehyde, which was used immediately in the next step without further purification. To a stirred suspension of LiCl (230 mg, 5.4 mmol) in MeCN (5 mL) under argon, were added (EtO)₂P(O)CH₂CO₂Bn (1.5 mL, 5.4 mmol) and (ⁱPr)₂NEt (DIPEA) (0.94 mL, 5.4 mmol) at 0 °C. After 20 min, the above aldehyde in MeCN (15 mL) was added to the mixture at 0 °C, and the mixture was stirred at this temperature for 8 h. The mixture was concentrated under reduced pressure, and the residue was extracted with EtOAc. The extract was washed successively with saturated aqueous citric acid and H₂O and dried over MgSO₄. Concentration under reduced pressure followed by chromatography over silica gel with CHCl₃/MeOH (40:1) gave the title compound **9** (1.0 g, 1.5 mmol, 67% yield from **8**) as a colorless oil.

[α]²³_D −10.1 (*c* 1.49, CHCl₃). ¹H NMR (270 MHz, CDCl₃) δ: 1.63 (4H, br m, 1, 2-CH₂), 2.17 (3H, s, Ar-*p*-Me), 2.64 (6H, s, Ar-*o*-Me), 3.20 (2H, br m, 3-CH₂), 3.22 (1H, br, 2-H), 3.61 (1H, br, 3-H), 5.15 (2H, s, CH₂), 6.18 (1H, dd, *J* = 15.7, 0.8 Hz, CH=), 6.22 (3H, br, guanidino), 6.66 (1H, dd, *J* = 15.5, 6.9 Hz, CH=), 6.88 (2H, s, ArH), 7.34 (5H, s, ArH), 7.56−7.60 (1H, m, ArH), 7.71−7.79 (2H, m, ArH), 8.13−8.17 (1H, m, ArH). *m/z* (ISMS): 670.5 (MH⁺). Found (FAB-HRMS): 670.2019. Calcd for C₃₁H₃₆O₈N₅S₂ (MH⁺): 670.2005.

Phenylmethyl 8-[[Imino[[(2,4,6-trimethylphenyl)sul-fonyl]amino]methyl]amino]-5(*S*)-[[(2-nitrophenyl)sulfo-nyl]amino]-2(*R*)-(naphthylmethyl)oct-3-enoate [Ns-L-Arg-(Mts)-ψ[(*E*)-CH=CH]-L-Nal-OBn], 10. To a stirred solution of CuCN (219 mg, 2.45 mmol) and LiCl (207 mg, 4.89 mmol) in dry THF (3.0 mL) under argon at −78 °C, was added dropwise 0.5 M (2-naphthylmethyl)zincbromide in THF solu-tion (4.9 mL, 2.45 mmol), and the mixture was stirred at 0 °C for 10 min. A solution of enoate **9** (273 mg, 0.408 mmol) in dry THF (9.0 mL) was added dropwise to the above mixture at −78 °C with stirring, and the stirring was continued for 30 min followed by quenching with 10 mL of a 1:1 saturated aqueous NH₄Cl/28% NH₄OH solution. The mixture was ex-tracted with Et₂O, and the extract was washed with saturated aqueous NH₄Cl and brine and dried over MgSO₄. Concentra-tion under reduced pressure gave an oily residue, which was purified by chromatography over silica gel with *n*-hexane/EtOAc (1:2) to yield 273 mg (0.337 mmol, 83% yield from **9**) of compound **10** as a yellow oil. [α]³³_D −80.9 (*c* 0.61, CHCl₃). ¹H NMR (270 MHz, CDCl₃) δ: 1.35 (2H, br m, 2-CH₂), 1.55 (2H, br m, 1-CH₂), 2.04 (3H, s, Ar-*p*-Me), 2.26 (6H, s, Ar-*o*-Me), 2.97 (2H, br, CH₂), 2.98 (2H, br m, 3-CH₂), 3.20−3.25 (1H, m, 2-H), 3.90 (1H, br, 5-H), 4.93 (2H, s, CH₂), 5.24 (1H, dd, *J* = 15.5, 6.9 Hz, CH=), 5.50 (1H, dd, *J* = 15.4, 8.4 Hz, CH=), 5.67 (1H, d, *J* = 4.6 Hz, NH), 5.95 (3H, br, guanidino), 6.89 (2H, s, ArH), 7.05−7.28 (7H, m, ArH), 7.42−7.77 (9H, m, ArH), 7.96−8.00 (1H, m, ArH). *m/z* (ISMS): 814.0 (MH⁺). Found (FAB-HRMS): 812.2803. Calcd for C₄₂H₄₆O₈N₅S₂ (MH⁺): 812.2788.

Phenylmethyl 5(*S*)-[(Fluoren-9-ylmethoxy)carbonyl-amino]-8-[[imino[[(2,4,6-trimethylphenyl)sulfonyl]ami-no]methyl]amino]-2(*R*)-(2-naphthylmethyl)oct-3-enoate [Fmoc-L-Arg(Mts)-ψ[(*E*)-CH=CH]-L-Nal-OBn], 11. To a stirred solution of enoate **10** (81 mg, 0.10 mmol) in DMSO/MeCN (1:49, 5 mL), were added thiophenol (31 μL, 0.3 mmol) and K₂CO₃ (55 mg, 0.4 mmol) at room temperature, and the mixture was stirred at 50 °C for 1 h. The solution was filtered, and the filtrate was concentrated under reduced pressure. The residue was extracted with EtOAc, washed with brine, and dried over MgSO₄. Concentration under reduced pressure gave an oily residue, which was dissolved in THF/H₂O (1:1, 50 mL). Fmoc-OSu (33 mg, 0.1 mmol) and Et₃N (27 μL, 0.19 mmol) were added to the above solution at 0 °C. After being stirred for 6 h, the mixture was acidified with 0.1 M HCl and then extracted with EtOAc. The extract was washed with 0.1 M HCl and brine and dried over MgSO₄. Concentration under reduced pressure followed by chromatography over silica gel with *n*-hexane/EtOAc (1:2) gave the title compound **11** (60 mg, 70.9 μmol, 71% yield from **10**) as a colorless oil.

[α]²⁹_D −11.2 (*c* 0.63, CHCl₃). ¹H NMR (270 MHz, CDCl₃) δ: 1.26 (4H, br m, 1, 2-CH₂), 2.18 (3H, s, Ar-*p*-Me), 2.63 (6H, s,

Ar-*o*-Me), 2.94 (2H, br, CH$_2$), 3.19 (2H, br m, 3-CH$_2$), 3.38 (1H, br, 2-H), 3.96 (1H, br, 5-H), 4.12 (1H, t, J = 5.8 Hz, ArH), 4.35 (2H, t, J = 5.94 Hz, CH$_2$), 4.82 (1H, br, NH), 5.01 (2H, s, CH$_2$), 5.24 (1H, dd, J = 15.0, 5.7 Hz, CH=), 5.64 (1H, dd, J = 14.4, 7.8 Hz, CH=), 6.16 (3H, br, guanidino), 6.81 (2H, s, ArH), 7.08−7.28 (8H, m, ArH), 7.33−7.42 (4H, m, ArH), 7.42−7.54 (3H, m, ArH), 7.64−7.74 (5H, m, ArH). *m/z* (ISMS): 850.0 (MH$^+$). Found (FAB-HRMS): 849.3664. Calcd for C$_{51}$H$_{53}$O$_6$N$_4$S$_2$ (MH$^+$): 849.3686.

5(*S*)-[(Fluoren-9-ylmethoxy)carbonylamino]-8-[[imino-[[(2, 4, 6-trimethylphenyl)sulfonyl]amino]methyl]amino]-2(*R*)-(2-naphthylmethyl)oct-3-enoic Acid [Fmoc-L-Arg-(Mts)-ψ[(*E*)-CH=CH]-L-Nal-OH], 12. The enoate 11 (30 mg, 0.037 mmol) was dissolved in TFA (10 mL), and thioanisole (500 μL), *m*-cresol (200 μL), and 1,2-ethanedithiol (100 μL) were added to the solution at 0 °C, and the mixture was stirred for 12 h at room temperature. The mixture was concentrated under reduced pressure and extracted with EtOAc. The extract was washed with brine and dried over MgSO$_4$. Concentration under reduced pressure followed by chromatography over silica gel with *n*-hexane/EtOAc (1:4) gave the title compound 12 (28 mg, 0.036 mmol, 98% yield from 11) as a colorless oil.

[α]^{23}$_D$ −15.2 (*c* 0.07, CHCl$_3$). ^{1}H NMR (600 MHz, CDCl$_3$) δ: 1.25 (4H, br m, 1, 2-CH$_2$), 2.20 (3H, s, Ar-*p*-Me), 2.62 (6H, s, Ar-*o*-Me), 2.86 (2H, br, CH$_2$), 3.05 (2H, br m, 3-CH$_2$), 3.49 (1H, br, 2-H), 3.68 (1H, br, 5-H), 4.10 (1H, br, ArH), 4.20−4.26 (2H, m, CH$_2$), 4.93 (1H, br, CH=), 5.34 (1H, br, CH=), 5.38 (1H, br, NH), 5.95 (1H, br, guanidino), 6.84 (2H, s, ArH), 7.20−7.41 (7H, m, ArH), 7.48−7.57 (3H, m, ArH), 7.65−7.77 (5H, m, ArH). *m/z* (ISMS): 760.0 (MH$^+$). Found (FAB-HRMS): 759.3228. Calcd for C$_{44}$H$_{47}$O$_6$N$_4$S$_2$ (MH$^+$): 759.3216.

Phenylmethyl 8-[[Imino[[(2, 4, 6-trimethylphenyl)sulfonyl]amino]methyl]amino]-5(*S*)-[[(2-nitrophenyl)sulfonyl]amino]-2(*S*)-(naphthylmethyl)oct-3-enoate [Ns-L-Arg(Mts)-ψ[(*E*)-CH=CH]-D-Nal-OBn], 14. To a stirred solution of enoate 9 (500 mg, 0.75 mmol) in CHCl$_3$ (5 mL) was added dropwise MSA (435 μL, 6.7 mmol) at room temperature with stirring, and the stirring was continued for 20 min. The mixture was extracted with EtOAc, and the extract was washed successively with aqueous 5% citric acid, water, aqueous 5% NaHCO$_3$, and water and dried over MgSO$_4$. Concentration under reduced pressure gave an oily residue of the crude mesylate 13, which was used directly in the following step without further purification. To a stirred slurry of CuCN (269 mg, 3.0 mmol) in dry THF (5 mL) under argon at −78 °C was added dropwise (2-naphthylmethyl)zincbromide in THF solution (6.0 mL, 3.0 mmol), and the mixture was stirred at 0 °C for 15 min followed by addition of BF$_3$·Et$_2$O (369 μL, 3.0 mmol) at −78 °C and then stirred at −78 °C for 15 min. To the mixture at −78 °C with stirring was added by syringe a solution of the crude mesylate 13 in THF (10 mL), and the stirring was continued at −78 °C for 1 h followed by quenching with saturated aqueous NH$_4$Cl and aqueous 28% NH$_4$OH (1:1) at 0 °C. The mixture was allowed to warm to room temperature and extracted with Et$_2$O. The extract was washed with H$_2$O, dried over MgSO$_4$, and concentrated under reduced pressure. The residue was purified by chromatography over silica gel with *n*-hexane/EtOAc (1:2) to give 408 mg (0.50 mmol, 67% from 9) of protected EADI 14 as a yellow oil. [α]^{32}$_D$ −41.7 (*c* 0.60, CHCl$_3$). ^{1}H NMR (270 MHz, CDCl$_3$) δ: 1.54 (4H, br m, 1, 2-CH$_2$), 2.25 (3H, s, Ar-*p*-Me), 2.66 (6H, s, Ar-*o*-Me), 2.86 (2H, br m, 3-CH$_2$), 2.98−3.06 (2H, m, CH$_2$), 3.15−3.23 (1H, m, 2-H), 3.78−3.88 (1H, m, 5-H), 4.98 (2H, s, CH$_2$), 5.09 (1H, dd, J = 15.5, 8.0 Hz, CH=), 5.49 (1H, dd, J = 15.5, 8.2 Hz, CH=), 5.57 (1H, d, J = 8.4 Hz, NH), 6.09 (3H, br, guanidino), 6.89 (2H, s, ArH), 7.10−7.26 (7H, m, ArH), 7.37−7.76 (9H, m, ArH), 7.95−7.98 (1H, m, ArH). *m/z* (ISMS): 814.0 (MH$^+$). Found (FAB-HRMS): 812.2775. Calcd for C$_{42}$H$_{46}$O$_8$N$_5$S$_2$ (MH$^+$): 812.2788.

Phenylmethyl 5(*S*)-[(Fluoren-9-ylmethoxy)carbonylamino]-8-[[imino[[(2,4,6-trimethylphenyl)sulfonyl]amino]methyl]amino]-2(*S*)-(2-naphthylmethyl)oct-3-enoate [Fmoc-L-Arg(Mts)-ψ[(*E*)-CH=CH]-D-Nal-OBn], 15. By use of a procedure identical with that described for the preparation

of 11 from 10, the enoate 14 (30 mg, 37 μmol) was converted into 28 mg (36 μmol, 98% yield from 14) of the title compound 15 as a colorless oil.

[α]^{29}$_D$ −1.6 (*c* 0.61, CHCl$_3$). ^{1}H NMR (270 MHz, CDCl$_3$) δ: 1.14−1.30 (4H, br m, 1, 2-CH$_2$), 2.17 (3H, s, Ar-*p*-Me), 2.62 (6H, s, Ar-*o*-Me), 2.91 (2H, br m, 3-CH$_2$), 3.15−3.23 (2H, m, CH$_2$), 3.40 (1H, br, 2-H), 3.95 (1H, br, 5-H), 4.11 (1H, t, J = 6.5 Hz, ArH), 4.33 (2H, d, J = 5.7 Hz, CH$_2$), 4.85 (1H, d, J = 6.8 Hz, NH), 5.00 (2H, s, CH$_2$), 5.25 (1H, dd, J = 16.7, 6.8 Hz, CH=), 5.61 (1H, dd, J = 14.3, 7.6 Hz, CH=), 6.13 (3H, br, guanidino), 6.81 (2H, s, ArH), 7.09−7.27 (8H, m, ArH), 7.32−7.45 (4H, m, ArH), 7.46−7.56 (3H, m, ArH), 7.64−7.73 (5H, m, ArH). *m/z* (ISMS): 850.0 (MH$^+$). Found (FAB-HRMS): 849.3698. Calcd for C$_{51}$H$_{53}$O$_6$N$_4$S$_2$ (MH$^+$): 849.3686.

5(*S*)-[(Fluoren-9-ylmethoxy)carbonylamino]-8-[[imino-[[(2, 4, 6-trimethylphenyl)sulfonyl]amino]methyl]amino]-2(*S*)-(2-naphthylmethyl)oct-3-enoic Acid [Fmoc-L-Arg-(Mts)-ψ[(*E*)-CH=CH]-D-Nal-OH], 16. By use of a procedure identical with that described for the preparation of 12 from 11, the enoate 15 (153 mg, 0.19 mmol) was converted into 144 mg (0.19 mmol, 99% yield from 15) of the title compound 16 as a colorless oil.

[α]^{23}$_D$ 10.8 (*c* 0.19, CHCl$_3$). ^{1}H NMR (270 MHz, CDCl$_3$) δ: 1.24 (4H, br m, 1, 2-CH$_2$), 2.17 (3H, s, Ar-*p*-Me), 2.70 (6H, s, Ar-*o*-Me), 2.90 (2H, br m, 3-CH$_2$), 3.07 (2H, m, CH$_2$), 3.29 (1H, br, 2-H), 3.67 (1H, br, 5-H), 4.06 (1H, t, J = 8.2 Hz, ArH), 4.28 (2H, d, J = 5.9 Hz, CH$_2$), 5.12 (1H, d, J = 5.9 Hz, NH), 5.26 (1H, dd, J = 15.0, 5.8 Hz, CH=), 5.59 (1H, dd, J = 15.0, 8.0 Hz, CH=), 6.19 (3H, br, guanidino), 6.80 (2H, s, ArH), 7.18−7.40 (7H, m, ArH), 7.46−7.54 (3H, m, ArH), 7.59−7.70 (5H, m, ArH). *m/z* (ISMS): 760.0 (MH$^+$). Found (FAB-HRMS): 759.3201. Calcd for C$_{44}$H$_{47}$O$_6$N$_4$S$_2$ (MH$^+$): 759.3216.

H-D-Tyr(O^{t}Bu)-Arg(Pbf)-Arg(Mts)-ψ[(*E*)-CH=CH]-Nal-Gly-NHNHCO−Wang Resin. *p*-Nitrophenyl carbonate Wang resin 33 (Calbiochem-Novabiochem Japan, Ltd., Tokyo, Japan, 0.93 mmol/g, 323 mg, 0.3 mmol) was treated with NH$_2$NH$_2$·H$_2$O (146 μL, 3.0 mmol) in DMF (3 mL) at room temperature for 2 h to give a hydrazide linker 34. Protected peptide−resins were manually constructed by Fmoc-based solid-phase peptide synthesis. ^{t}Bu for Tyr and Mts or Pbf for Arg were employed for side-chain protection. Fmoc deprotection was achieved by 20% piperidine in DMF (1 min × 2 and 15 min × 1). Fmoc−amino acids including EADIs or RADIs were condensed to free amino groups by treatment with 3 equiv of reagents (Fmoc−amino acid, *N*,*N*′-diisopropylcarbodiimide (DIPCDI) and HOBt·H$_2$O) in DMF for 1.5 h.

***cyclo*(-D-Tyr-Arg-Arg-ψ[(*E*)-CH=CH]-Nal-Gly-)·2TFA (37a).** The protected 37a resin (34 mg, 0.025 mmol) was treated with TFA (0.5 mL) in CHCl$_3$ (4.5 mL) at room temperature for 2 h, and the mixture was filtered. Concentration of the filtrate under reduced pressure gave a crude hydrazide (H-D-Tyr-Arg(Pbf)-Arg(Mts)-ψ[(*E*)-CH=CH]-Nal-Gly-NHNH$_2$) as a colorless powder. To a stirred solution of the hydrazide in DMF (1 mL) were added a solution of 4 M HCl in DMF (16.6 μL, 75 μmol) and isoamyl nitrite (40 μL, 0.20 mmol) at −30 °C. After being stirred at −10 °C for 20 min, the mixture was diluted with precooled DMF (50 mL). To the above solution was added DIPEA (191 μL, 1.1 mmol) at −30 °C, and the mixture was stirred for 48 h at −20 °C. Concentration under reduced pressure gave a yellow oil (crude *cyclo*(-D-Tyr-Arg(Pbf)-Arg(Mts)-ψ[(*E*)-CH=CH]-Nal-Gly-)). To the protected cyclic peptide were added *m*-cresol (0.4 mL, 3.6 mmol), 1, 2-ethanedithiol (160 μL, 1.9 mmol), thioanisole (1.0 mL, 8.5 mmol), TFA (10 mL), and bromotrimethylsilane (1.2 mL, 9.1 mmol) at 0 °C, and the stirring was continued at room temperature for 12 h. Concentration under reduced pressure and purification by preparative HPLC gave the cyclic pseudo-peptide 37a (8.5 mg, 36% yield from protected 37a resin) as a freeze-dried powder.

[α]^{27}$_D$ −53.3 (*c* 0.24, H$_2$O). t_R = 28.6 min (linear gradient of MeCN in H$_2$O, 10 to 40% over 30 min). *m/z* (ISMS): 714.0 (MH$^+$). Found (FAB-HRMS): 713.3879. Calcd for C$_{37}$H$_{49}$O$_5$N$_{10}$ (MH$^+$): 713.3887.

***cyclo*(-D-Tyr-Arg-Arg-ψ[(*E*)-CH=CH]-D-Nal-Gly-)· 2TFA (37f).** By use of a procedure identical with that described

for the preparation of **37a**, the protected **37f** (34 mg, 0.025 mmol) was converted into 9.8 mg (10.5 μmol, 42%) of the title compound **37f**, as a freeze-dried powder.

$[\alpha]^{26}{}_D$ −32.0 (c 0.13, H$_2$O). t_R = 28.9 min (linear gradient of MeCN in H$_2$O, 10 to 40% over 30 min). *m/z* (ISMS): 714.0 (MH$^+$). Found (FAB-HRMS): 713.3903. Calcd for C$_{37}$H$_{49}$O$_5$N$_{10}$ (MH$^+$): 713.3887.

(*tert*-Butoxy)-*N*-[2(*R,S*)-hydroxy-1(*S*)-(2-naphthylmeth-yl)but-3-enyl]formamide, 20. To a stirred solution of Boc-Nal-OMe **19** (4.0 g, 12.2 mmol) in CH$_2$Cl$_2$ (100 mL) was added dropwise a solution of DIBAL-H in toluene (1.0 M, 24.4 mL, 24.4 mmol) at −78 °C under argon, and the mixture was stirred at −78 °C for 2 h. To the solution was added dropwise a vinyl Grignard (CH$_2$=CHMgCl) reagent in THF (12.6 mL, 36.6 mmol) at −78 °C, and the mixture was stirred for 6 h with warming to 0 °C. The reaction was quenched with saturated aqueous citric acid at −78 °C, and organic solvents were concentrated under reduced pressure. The residue was extracted with EtOAc, and the extract was washed successively with saturated aqueous citric acid, saturated aqueous NaHCO$_3$, and brine and dried over MgSO$_4$. Concentration under reduced pressure followed by chromatography over silica gel with EtOAc/*n*-hexane (3:1) gave a mixture of *threo*- and *erythro*-allyl alcohols **20** (1.4 g, 35% yield from **19**) as a colorless oil. The mixture of diastereoisomer was used in the following step without further purification.

^{1}H NMR (270 MHz, CDCl$_3$) δ: 1.24−1.36 (9H, br, *tert*-Bu), 2.90−2.94 (1H, br, 2-H), 3.00−3.03 (2H, br, CH$_2$), 3.86−3.94 (1H, br, 1-H), 4.95−5.01 (1H, br, NH), 5.13−5.17 (1H, m, C*H*H=), 5.22−5.29 (1H, m, CH*H*=), 5.82−5.94 (1H, m, CH=), 7.38−7.43 (3H, m, ArH), 7.68−7.80 (4H, m, ArH). *m/z* (ISMS): 328.5 (MH$^+$). Found (FAB-HRMS): 328.1921. Calcd for C$_{20}$H$_{26}$O$_3$N (MH$^+$): 328.1913.

1(*S*)-[1-[(*tert*-Butoxy)carbonylamino]-2-(naphthyl)eth-yl]prop-2(*R, S*)-enyl Acetate, 21. To a stirred solution of allyl alcohol **20** (8.5 g, 26.0 mmol) in CHCl$_3$ (10 mL), were added acetic anhydride (11.0 mL, 117 mmol) and pyridine (18.9 mL, 234 mmol) at 4 °C, and the mixture was stirred at room temperature for 6 h. The mixture was concentrated under reduced pressure. The residue was extracted with EtOAc, and the extract was washed with aqueous 5% NaHCO$_3$, aqueous 1 M HCl, and brine and dried over MgSO$_4$. Concentration under reduced pressure followed by chromatography over silica gel with EtOAc/*n*-hexane (2:1) gave acetates **21** (5.7 g, 59% yield from **20**) as a colorless oil.

^{1}H NMR (270 MHz, CDCl$_3$) δ: 1.29−1.37 (9H, br, *tert*-Bu), 2.06−2.08 (3H, br, Me), 2.80−2.84 (1H, br, 2-H), 2.89−2.95 (2H, br, CH$_2$), 4.14−4.20 (1H, br, 1-H), 4.74−4.78 (1H, br, NH), 5.20−5.24 (1H, br m, C*H*H=), 5.25−5.30 (1H, br m, CH*H*=), 5.74−5.80 (1H, m, CH=), 7.30−7.42 (3H, m, ArH), 7.60−7.76 (4H, m, ArH). *m/z* (ISMS): 370.5 (MH$^+$). Found (FAB-HRMS): 370.2016. Calcd for C$_{22}$H$_{28}$O$_4$N (MH$^+$): 370.2018.

tert-Butyl 4(*R,S*)-Acetoxy-5(*S*)-[(*tert*-butoxy)carbonyl-amino]-6-(2-naphthyl)hex-2-enoate, 22. To a solution of acetate **21** (5.7 g, 15.4 mmol) in CH$_2$Cl$_2$ (40 mL) was bubbled O$_3$ gas at −78 °C until a blue color persisted. To the above solution, was added Me$_2$S (11 mL, 154 mmol), and the mixture was stirred for 30 min. The mixture was dried over MgSO$_4$. Concentration under reduced pressure gave an oily residue of a crude aldehyde, which was used immediately in the next step without further purification. To a stirred suspension of LiCl (1.57 g, 37 mmol) in MeCN (10 mL) under argon were added (EtO)$_2$P(O)CH$_2$CO$_2$^{t}Bu (8.7 mL, 37 mmol) and DIPEA (6.4 mL, 37 mmol) at 0 °C. After 20 min, the above aldehyde in MeCN (20 mL) was added to the above mixture at 0 °C, and the mixture was stirred at this temperature for 8 h. The mixture was concentrated under reduced pressure, and the residue was extracted with EtOAc. The extract was washed successively with saturated aqueous citric acid and H$_2$O and dried over MgSO$_4$. Concentration under reduced pressure followed by chromatography over silica gel with EtOAc/*n*-hexane (1:2) gave enoates **22** (2.1 g, 29% yield from **21**) as a white amorphous semisolid.

Found: C, 68.97; H, 7.60; N, 2.92. C$_{27}$H$_{35}$O$_6$N Calcd: C, 69.06; H, 7.51; N, 2.98. ^{1}H NMR (270 MHz, CDCl$_3$) δ: 1.34−1.38 (9H, br, *tert*-Bu), 1.43−1.47 (9H, br, *tert*-Bu), 2.13−2.17 (3H, br, Me), 2.91−2.99 (2H, br, CH$_2$), 4.22−4.32 (1H, br, 5-H), 4.71−4.77 (1H, br, 4-H), 5.42−5.46 (1H, br, NH), 5.79−5.99 (1H, m, CH=), 6.70−6.83 (1H, m, CH=), 7.43−7.49 (3H, m, ArH), 7.77−7.82 (4H, m, Ar). *m/z* (FAB-LRMS): 468 [(M−H)$^-$], 305, 199, 153, 151, and 46 (base peak). Found (FAB-HRMS): 468.2375. Calcd for C$_{27}$H$_{34}$O$_6$N [(M−H)$^-$]: 468.2386.

tert-Butyl 5(*S*)-[(*tert*-Butoxy)carbonylamino]-6-(2-naph-thyl)hex-3-enoate (Boc-L-Nal=Gly-O^{t}Bu), 23. To a stirred slurry of Sm (900 mg, 6.0 mmol) in dry THF (20 mL) under argon at room temperature was added a solution of CH$_2$I$_2$ (322 μL, 4.0 mmol) in dry THF (20 mL), and the slurry was stirred at room temperature for 2 h until a dark green color persisted. To a stirred solution of enoate **22** (600 mg, 1.3 mmol) in dry THF (16 mL) in the other vessel were added *tert*-BuOH (8 mL, excess) and the above SmI$_2$ solution (38 mL, 3.8 mmol) under argon at room temperature, and the mixture was stirred for 1 h. The reaction was then quenched with saturated aqueous NH$_4$Cl (10 mL) at 4 °C, and the mixture was extracted with Et$_2$O (20 mL). The extract was washed with saturated aqueous NH$_4$Cl and brine and dried over MgSO$_4$. Concentration under reduced pressure followed by chromatography over silica gel with EtOAc/*n*-hexane (1:4) gave the enoate **23** (530 mg, 95% yield from **22**) as white crystals.

Mp: 80−82 °C (from *n*-hexane). Found: C, 73.17; H, 8.17; N, 3.39. C$_{25}$H$_{33}$O$_4$N Calcd: C, 72.96; H, 8.08; N, 3.40. $[\alpha]^{25}{}_D$ 11.00 (c 1.09, CHCl$_3$). ^{1}H NMR (400 MHz, CDCl$_3$) δ: 1.37 (9H, s, *tert*-Bu), 1.41 (9H, s, *tert*-Bu), 2.93 (2H, d, *J* = 6.4 Hz, 6-CH$_2$), 2.98 (2H, d, *J* = 6.8 Hz, 2-CH$_2$), 4.48−4.59 (1H, br, NH), 5.43 (1H, t, *J* = 11.2 Hz, 5-H), 5.55 (1H, dd, *J* = 15.6, 5.6 Hz, CH=), 5.61−5.69 (1H, br, CH=), 7.31−7.46 (3H, m, ArH), 7.60−7.62 (1H, br, ArH), 7.74−7.78 (3H, m, ArH). *m/z* (ISMS): 412.0 (MH$^-$). Found (FAB-HRMS): 412.2491. Calcd for C$_{25}$H$_{34}$O$_4$N (MH$^+$): 412.5418.

5(*S*)-[(Fluoren-9-ylmethoxy)carbonylamino]-6-(2-naph-thyl)hex-3-enoic Acid (Fmoc-L-Nal=Gly-OH), 24. The enoate **23** (1.79 g, 4.35 mmol) was dissolved in TFA (30 mL), anisole (472 μL, 4.35 mmol) was added to the solution at 4 °C, and the mixture was stirred at room temperature for 2 h. The mixture was concentrated under reduced pressure and dissolved in THF and H$_2$O (1:1 (v/v) 20 mL). To the stirred solution were added Fmoc-OSu (1.47 g, 4.35 mmol) and Et$_3$N (10 mL, 71.7 mmol) at 4 °C, and the mixture was stirred at room temperature for 8 h. The mixture was acidified with aqueous 1 M HCl and was extracted with EtOAc. The extract was washed with aqueous 0.1 M HCl and brine and dried over MgSO$_4$. Concentration under reduced pressure followed by chromatography over silica gel with EtOAc/*n*-hexane (3:1) gave the enoic acid **24** (1.61 g, 78% yield from **23**) as white crystals.

Mp: 134−136 °C (from *n*-hexane). $[\alpha]^{23}{}_D$ −2.75 (c 0.73, CHCl$_3$). ^{1}H NMR (400 MHz, CDCl$_3$) δ: 2.96 (2H, br, 6-CH$_2$), 3.03 (2H, br, 2-CH$_2$), 4.14 (1H, t, *J* = 6.6 Hz, ArH), 4.32 (1H, dd, *J* = 14.9, 7.2 Hz, CH=), 4.38 (1H, m, CH=) 4.54 (1H, d, *J* = 7.6 Hz, CH$_2$), 4.81 (1H, br, 5-H), 5.62 (1H, br, NH), 7.18−7.28 (2H, m, ArH), 7.30−7.52 (5H, m, ArH), 7.57−7.63 (2H, m, ArH), 7.70−7.79 (6H, m, ArH). *m/z* (ISMS): 478.0 (MH$^+$). Found (FAB-HRMS): 478.2016. Calcd for C$_{31}$H$_{28}$O$_4$N (MH$^+$): 478.2018.

H-D-Tyr(O^{t}Bu)-Arg(Pbf)-Arg(Pbf)-Nal-ψ[(*E*)-CH=CH]-Gly-NHNHCO−Wang Resin. On the hydrazide resin, were coupled successively Fmoc-D-Tyr(O^{t}Bu)-OH, Fmoc-Nal-ψ[(*E*)-CH=CH]-Gly-OH, and Fmoc-Arg(Pbf)-OH by use of the procedure identical with that described for the preparation of H-D-Tyr(O^{t}Bu)-Arg(Pbf)-Arg(Mts)-ψ[(*E*)-CH=CH]-Nal-Gly-NHNHCO−Wang resin to afford the protected **37c** resin.

***cyclo*(-D-Tyr-Arg-Arg-Nal-ψ[(*E*)-CH=CH]-Gly-)·2TFA (37c).** By use of a procedure identical with that described for the preparation of **37a**, the protected **37c** resin (173 mg, 0.13 mmol) was converted into 7.0 mg (7.4 μmol, 5.9%) of the title compound **37c**, as a freeze-dried powder.

$[\alpha]^{21}{}_D$ −43.1 (c 0.33, H$_2$O). t_R = 24.3 min (linear gradient of MeCN in H$_2$O, 10 to 40% over 30 min). *m/z* (ISMS): 713.0

(MH⁺). Found (FAB-HRMS): 713.3911. Calcd for C₃₇H₄₉O₅N₁₀ (MH⁺): 713.3887.

***tert*-Butyl 2(*S*)-[[2(*S*)-[(*tert*-butoxy)carbonyamino]-5-[[imino[[(2,4,6-trimethylphenyl)sulfonyl]amino]methyl]-amino]pentyl]amino]-3-(2-naphthyl) Propanoate [Boc-L-Arg(Mts)-ψ[CH₂−NH]-L-Nal-O′Bu], 26.** To a stirred solution of 25 (5.0 g, 10 mmol) in toluene/CH₂Cl₂ (1:1 (v/v), 50 mL) was added dropwise a solution of DIBAL-H in toluene (1.0 M, 60 mL, 60 mmol) at −50 °C under argon, and the mixture was stirred for 4 h at −78 °C. The reaction was quenched with saturated aqueous citric acid at −78 °C, and the organic solvents were concentrated under reduced pressure. The residue was extracted with EtOAc, and the extract was washed successively with saturated aqueous citric acid and brine and dried over MgSO₄. Concentration under reduced pressure gave a crude aldehyde (Boc-Arg(Mts)-H), which was used in the following step without further purification. To the stirred solution of Boc-Arg(Mts)-H in ClCH₂CH₂Cl/DMF (1:6 (v/v), 100 mL), were added H-L-Nal-O′Bu (5.4 g, 20 mmol) and AcOH (1.1 mL, 20 mmol) at 4 °C and stirred for 10 min. NaBH(OAc)₃ (6.4 g, 30 mmol) was added to the above mixture at 4 °C and stirred for 8 h with warming to room temperature. The mixture was concentrated under reduced pressure, and the residue was extracted with CHCl₃. The extract was washed with aqueous 5% NaHCO₃ and brine and dried over MgSO₄. Concentration under reduced pressure gave an oily residue, which was purified by chromatography over silica gel with CHCl₃/MeOH (39:1) to yield 3.4 g (4.9 mmol, 49% yield from 25) of compound 26 as a yellow oil.

[α]²³_D 4.08 (*c* 1.96, CHCl₃). ¹H NMR (270 MHz, CDCl₃) δ: 1.24 (9H, s, *tert*-Bu), 1.32 (9H, s, *tert*-Bu), 1.55 (2H, br m, 4-CH₂), 1.74 (2H, br m, 3-CH₂), 2.25 (3H, s, Ar-*p*-Me), 2.67 (6H, s, Ar-*o*-Me), 3.08 (2H, br m, 5-CH₂), 3.20 (2H, br, 3-CH₂), 3.34 (2H, br, 1-CH₂), 3.62 (1H, br, 2-H), 3.82 (1H, br, 2-H), 3.99 (1H, br, NH), 5.95 (1H, br, NH), 6.61 (3H, br, guanidino), 6.87 (2H, s, Ar-*m*-H), 7.36−7.44 (3H, m, ArH), 7.67−7.75 (4H, m, ArH). *m/z* (ISMS): 697.0 (MH⁺). Found (FAB-HRMS): 696.3812. Calcd for C₃₇H₅₄O₆N₅S (MH⁺): 696.3795.

***tert*-Butyl 2(*S*)-[*N*-[2(*S*)-[(*tert*-Butoxy)carbonylamino]-5-[[imino[[(2,4,6-trimethylphenyl)sulfonyl]amino]methyl]-amino]pentyl](phenylmethoxy)carbonylamino]-3-(2-naphthyl)propanoate [Boc-Arg(Mts)-ψ[CH₂−N(Cbz)]-Nal-O′Bu], 27.** To a stirred solution of propanoate 26 (1.4 g, 2.0 mmol) in DMF (100 mL) at 4 °C, were added Cbz-Cl (0.69 g, 4.0 mmol) and Et₃N (560 μL, 4.0 mmol) and stirred at room temperature for 8 h. The mixture was concentrated under reduced pressure and extracted with EtOAc. The extract was washed with saturated aqueous citric acid, saturated aqueous NaHCO₃, and brine and dried over MgSO₄. Concentration under reduced pressure followed by chromatography over silica gel with EtOAc/*n*-hexane (1:1) gave the title compound 27 (1.6 g, 77% yield from 26) as a yellow oil.

[α]²³_D −36.44 (*c* 0.67, CHCl₃). ¹H NMR (270 MHz, CDCl₃) δ: 1.39 (9H, s, *tert*-Bu), 1.42 (9H, s, *tert*-Bu), 1.47 (2H, s, 4-CH₂), 1.64 (2H, br, 3-CH₂), 2.42 (3H, s, Ar-*p*-Me), 2.65 (6H, s, Ar-*o*-Me), 2.98 (2H, br, 5-CH₂), 3.27 (2H, br, 3-CH₂), 3.31 (2H, br, 1-CH₂), 3.40 (1H, br, 2-H), 4.24 (1H, br, 2-H), 5.08 (2H, s, CH₂), 5.90 (1H, br, NH), 6.13 (3H, br, guanidino), 6.86 (2H, s, Ar-*m*-H), 7.26 (5H, s, ArH), 7.31−7.46 (3H, m, ArH), 7.54−7.75 (4H, m, ArH). *m/z* (ISMS): 831.5 (MH⁺). Found (FAB-HRMS): 830.4153. Calcd for C₄₅H₆₀O₈N₅S (MH⁺): 830.4163.

2(*S*)-[*N*-[2(*S*)-[(Fluoren-9-ylmethoxy)carbonylamino]-5-[[imino[[(2,4,6-trimethylphenyl)sulfonyl]amino]methyl]-amino]pentyl](phenylmethoxy)carbonylamino]-3-(2-naphthyl)propanoic Acid [Fmoc-Arg(Mts)-ψ[CH₂−N(Cbz)]-Nal-OH], 28. The propanoate 27 (1.3 g, 1.57 mmol) was dissolved in TFA (30 mL), anisole (170 μL, 1.57 mmol) was added to the solution at 4 °C, and the mixture was stirred at room temperature for 2 h. The mixture was concentrated under reduced pressure and dissolved in THF and H₂O (1:1 (v/v) 100 mL). To the stirred solution were added Fmoc-OSu (530 mg, 1.57 mmol) and Et₃N (10 mL, 71.7 mmol) at 4 °C, and the mixture was stirred at room temperature for 8 h. The mixture

was acidified with aqueous 1 M HCl and extracted with EtOAc. The extract was washed with aqueous 0.1 M HCl and brine and dried over MgSO₄. Concentration under reduced pressure followed by chromatography over silica gel with EtOAc/*n*-hexane (4:1) gave the propanoic acid 28 (1.39 g, 99% yield from 27) as white crystals.

Mp: 156−158 °C (from *n*-hexane). [α]²⁴_D −8.17 (*c* 1.96, CHCl₃). ¹H NMR (270 MHz, CDCl₃) δ: 1.85 (2H, br, 4-CH₂), 1.93 (2H, br; 3-CH₂), 2.11 (3H, s, Ar-*p*-Me), 2.47 (6H, s, Ar-*o*-Me), 3.03 (2H, br, 5-CH₂), 3.22 (2H, br, 3-H), 3.37 (2H, br, 1-CH₂), 4.08 (1H, br, ArH), 4.15 (2H, br, CH₂), 4.30 (1H, br, 2-H), 5.16 (1H, br, NH), 6.36 (3H, br, guanidino), 6.83 (2H, s, Ar-*m*-H) 7.25 (5H, s, ArH), 7.29−7.40 (6H, m, ArH), 7.50−7.83 (9H, m, ArH). *m/z* (ISMS): 897.0 (MH⁺). Found (FAB-HRMS): 896.3693. Calcd for C₅₁H₅₄O₈N₅S (MH⁺): 896.3710.

H-D-Tyr(O′Bu)-Arg(Pbf)-Arg(Mts)-ψ[CH₂−NH]-Nal-Gly-NHNHCO−Wang Resin. On the hydrazide resin were coupled successively Fmoc-Gly-OH, Fmoc-Arg-ψ[CH₂−N(Cbz)]-Nal-OH, Fmoc-Arg(Pbf)-OH, and Fmoc-D-Tyr(O′Bu)-OH by use of a procedure identical with that described for the preparation of H-D-Tyr(O′Bu)-Arg(Pbf)-Arg(Mts)-ψ[(*E*)-CH=CH]-Nal-Gly-NHNHCO−Wang resin to afford the protected 37b resin.

***cyclo*(-D-Tyr-Arg-Arg-ψ[CH₂−NH]-Nal-Gly-)·3TFA (37b).** By use of a procedure identical with that described for the preparation of 37a, the protected 37b (200 mg, 0.15 mmol) was converted into 0.6 mg (0.57 μmol, 0.86%) of the title compound 37b, as a freeze-dried powder.

[α]²¹_D −22.6 (*c* 0.27, H₂O). *t*_R = 19.3 min (linear gradient of MeCN in H₂O, 10 to 40% over 30 min). *m/z* (ISMS): 717.0 (MH⁺). Found (FAB-HRMS): 716.4016. Calcd for C₃₆H₄₉O₅N₁₁ (MH⁺): 716.3996.

***tert*-Butyl 2(*S*)-[[2-[(*tert*-Butoxy)carbonylamino]-3-(2-naphthyl)propyl]amino]acetate [Boc-L-Nal-ψ[CH₂−NH]-Gly-O′Bu], 30.** To a stirred solution of Boc-Nal-NMe(OMe) 29 (5.5 g, 15 mmol) in toluene/CH₂Cl₂ (1:1 (v/v) 50 mL) was added dropwise a solution of DIBAL-H in toluene (1.0 M, 62 mL, 62 mmol) at −78 °C under argon, and the mixture was stirred at −78 °C for 4 h. The reaction was quenched with saturated aqueous citric acid at −78 °C, and organic solvents were concentrated under reduced pressure. The residue was extracted with EtOAc, and the extract was washed successively with saturated aqueous citric acid and brine and dried over MgSO₄. Concentration under reduced pressure gave a crude aldehyde (Boc-Nal-H), which was used in the following step without further purification. To the stirred solution of Boc-Nal-H in ClCH₂CH₂Cl/DMF (1:6 (v/v), 200 mL), was added H-Gly-O′Bu·AcOH (5.8 g, 31 mmol) at 4 °C and stirred for 10 min. NaBH(OAc)₃ (9.8 g, 46 mmol) was added to the above mixture at 4 °C and stirred for 8 h with warming to room temperature. The mixture was concentrated under reduced pressure, and the residue was extracted with CHCl₃. The extract was washed with aqueous 5% NaHCO₃ and brine and dried over MgSO₄. Concentration under reduced pressure gave an oily residue, which was purified by chromatography over silica gel with CHCl₃ to yield 3.2 g (7.7 mmol, 50% yield from 29) of compound 30 as a yellow oil.

[α]²²_D −0.67 (*c* 4.47, CHCl₃). ¹H NMR (400 MHz, CDCl₃) δ: 1.38 (9H, s, *tert*-Bu), 1.47 (9H, s, *tert*-Bu), 2.87 (2H, br, CH₂), 3.02 (2H, br, 3-CH₂), 3.85−3.94 (2H, m, 1-CH₂), 4.09−4.21 (1H, m, 2-H), 5.44 (1H, br, NH), 6.45 (1H, br, NH), 7.29−7.36 (2H, m, Ar−H), 7.41−7.48 (2H, m, ArH), 7.60−7.62 (1H, m, ArH), 7.72−7.83 (2H, m, ArH). *m/z* (ISMS): 415.5 (MH⁺). Found (FAB-HRMS): 415.2594. Calcd for C₂₄H₃₅O₄N₂ (MH⁺): 415.2597.

***tert*-Butyl 2(*S*)-[*N*-[2-[(*tert*-Butoxy)carbonylamino]-3-(2-naphthyl)propyl](phenylmethoxy)carbonylamino]acetate [Boc-L-Nal-ψ[CH₂−N(Cbz)]-Gly-O′Bu], 31.** To a stirred solution of acetate 30 (5.0 g, 12.1 mmol) in DMF (100 mL) at 4 °C were added Cbz-Cl (20.6 g, 121 mmol) and DIPEA (21.7 mL, 121 mmol), and the mixture was stirred at room temperature for 8 h. The mixture was concentrated under reduced pressure and extracted with EtOAc. The solution was washed with saturated aqueous citric acid, saturated aqueous NaH-CO₃, and brine and dried over MgSO₄. Concentration under

reduced pressure followed by chromatography over silica gel with EtOAc/n-hexane (1:2) gave the title compound **31** (4.0 g, 60% yield from **30**) as white crystals.

Mp: 107–109 °C (from n-hexane). Found: C, 70.01; H, 7.42 N, 4.98. Calcd for $C_{32}H_{40}O_6N_2$: C, 70.05; H, 7.35; N, 5.11. $[\alpha]^{23}_D$ −14.73 (c 0.48, CHCl$_3$). ^1H NMR (400 MHz, CDCl$_3$) δ: 1.34 (9H, s, $tert$-Bu), 1.35 (9H, s, $tert$-Bu), 2.94 (2H, br, CH$_2$), 3.37 (2H, br, 3-CH$_2$), 3.88 (2H, m, 1-CH$_2$), 4.05 (1H, m, 2-H), 4.94 (1H, br, NH), 5.13 (2H, s, CH$_2$), 7.28–7.33 (5H, br, ArH), 7.35–7.47 (3H, m, ArH), 7.74–7.81 (4H, m, ArH). m/z (ISMS): 549.5 (MH$^+$). Found (FAB-HRMS): 549.2953. Calcd for $C_{32}H_{41}O_6N_2$ (MH$^+$): 549.2965.

2(S)-[N-[2-[(Fluoren-9-ylmethoxy)carbonylamino]-3-(2-naphthyl)propyl](phenylmethoxy)carbonylamino]-acetic Acid [Fmoc-L-Nal-ψ[CH$_2$–N(Cbz)]-Gly-OH], 32. The acetate **31** (4.0 g, 7.29 mmol) was dissolved in TFA (30 mL), anisole (792 μL, 7.29 mmol) was added to the solution at 4 °C, and the mixture was stirred at room temperature for 2 h. The mixture was concentrated under reduced pressure and dissolved in THF and H$_2$O (1:1 (v/v) 100 mL). To the stirred solution, were added Fmoc-OSu (2.46 g, 7.29 mmol) and Et$_3$N (10 mL, 71.7 mmol) at 4 °C, and the mixture was stirred at room temperature for 8 h. The mixture was acidified with aqueous 1 M HCl and was extracted with EtOAc. The extract was washed with aqueous 0.1 M HCl and brine and dried over MgSO$_4$. Concentration under reduced pressure followed by chromatography over silica gel with CHCl$_3$/MeOH (39:1) gave the title compound **32** (4.20 g, 94% yield from **31**) as a yellow oil.

$[\alpha]^{23}_D$ −5.01 (c 4.79, CHCl$_3$). ^1H NMR (400 MHz, CDCl$_3$) δ: 2.99 (2H, d, J = 6.4 Hz, 3-CH$_2$), 3.41 (2H, s, CH$_2$), 4.00 (2H, br, 1-CH$_2$), 4.08 (1H, t, J = 6.6 Hz, Ar–H), 4.24 (1H, t, J = 6.2 Hz, 2-H), 4.27 (2H, br, CH$_2$), 5.05 (2H, s, CH$_2$), 5.53 (1H, d, J = 8.0 Hz, NH), 7.18 (5H, s, Ar–H) 7.30–7.50 (8H, m, ArH), 7.61–7.73 (7H, m, ArH). m/z (ISMS): 615.0 (MH$^+$). Found (FAB-HRMS): 615.2509. Calcd for $C_{38}H_{35}O_6N_2$ (MH$^+$): 615.2495.

H-D-Tyr(O'Bu)-Arg(Pbf)-Arg(Pbf)-Nal-ψ[CH$_2$–N(Cbz)]-Gly-NHNHCO–Wang Resin. On the hydrazide resin, were coupled successively Fmoc-D-Tyr(O'Bu)-OH, Fmoc-Nal-ψ[CH$_2$–N(Cbz)]-Gly-OH, and Fmoc-Arg(Pbf)-OH by use of a procedure identical with that described for the preparation of H-D-Tyr-(O'Bu)-Arg(Pbf)-Arg(Mts)-ψ[(E)-CH=CH]-Nal-Gly-NHNHCO–Wang resin to afford the protected **37d** resin.

***cyclo*(-D-Tyr-Arg-Arg-Nal-ψ[CH$_2$–NH]-Gly-)·3TFA (37d).** By use of a procedure identical with that described for the preparation of **37a**, the protected **37d** (173 mg, 0.13 mmol) was converted into 7.0 mg (7.4 μmol, 5.9%) of the title compound **37d**, as a freeze-dried powder.

$[\alpha]^{19}_D$ −58.0 (c 0.69, H$_2$O). t_R = 21.0 min (linear gradient of MeCN in H$_2$O, 10 to 40% over 30 min). m/z (ISMS): 717.0 (MH$^+$). Found (FAB-HRMS): 716.4003. Calcd for $C_{36}H_{49}O_5N_{11}$ (MH$^+$): 716.3996.

Cell Culture. Human T-cell lines, MT-4, and MOLT-4 cells were grown in RPMI 1640 medium containing 10% heat-inactivated fetal calf serum, 100 IU/mL penicillin, and 100 μg/mL streptomycin.

Virus. A strain of X4-HIV-1, HIV-1IIIB, was used for the anti-HIV assay. This virus was obtained from the culture supernatant of HIV-1 persistently infected MOLT-4/HIV-1IIIB cells and stored at −80 °C until used.

Anti-HIV-1 Assay. Anti-HIV-1 activity was determined based on the protection against HIV-1-induced cytopathogenicity in MT-4 cells. Various concentrations of test compounds were added to HIV-1-infected MT-4 cells at a multiplicity of infection (MOI) of 0.01 and placed in wells of a flat-bottomed microtiter tray (1.5 × 10^4 cells/well). After 5 days incubation at 37 °C in a CO$_2$ incubator, the number of viable cells was determined using the 3-(4,5-dimethylthiazol-2-yl)-2,5-diphenyltetrazolium bromide (MTT) method (EC$_{50}$).[48] Cytotoxicity of compounds was determined based on the viability of mock-infected cells using the MTT method (CC$_{50}$). 3'-Azido-3'-dideoxythymidine (AZT) was tested as a control.

[^{125}I]-SDF-1 Binding and Displacement. Stable CHO cell transfectants expressing CXCR4 variants were prepared as described previously.[49] CHO transfectants were harvested by treatment with trypsin/EDTA, allowed to recover in complete growth medium (MEM-α, 100 μg/mL penicillin, 100 μg/mL streptomycin, 0.25 μg/mL amphotericin B, 10% (v/v)) for 4–5 h, and then washed in cold binding buffer (PBS containing 2 mg/mL BSA). For ligand binding, the cells were resuspended in binding buffer at 1 × 10^7 cells/mL, and 100 μL aliquots were incubated with 0.1 nM of [^{125}I]-SDF-1 (PerkinElmer Life Sciences) for 2 h on ice under constant agitation. Free and bound radioactivities were separated by centrifugation of the cells through an oil cushion, and bound radioactivity was measured with a gamma counter (Cobra, Packard, Downers Grove, IL). Inhibitory activity of FC131 analogues was determined based on the inhibition of [^{125}I]-SDF-1-binding to CXCR4 transfectants (IC$_{50}$).

NMR Spectroscopy (37a and 37c). The peptide sample was dissolved in DMSO-d_6 at a concentration of 5 mM. ^1H NMR spectra of the peptides were recorded at 300 K. The assignments of the proton resonances were achieved by use of ^1H–^1H COSY spectra. $^3J(H^N, H^\alpha)$ coupling constants were measured from one-dimensional spectra. The mixing time for the nuclear Overhauser spectroscopy (NOESY) experiments was set at 400 ms. NOESY spectra were composed of 512 real points in the F2 dimension and 256 real points, which were zero-filled to 256 points in the F1 dimension, with 144 scans per t1 increment. The cross-peak intensities were evaluated by relative buildup rates of the cross peaks. Temperature dependence of the chemical shifts of all of the amide bonds was investigated in **37a** and **37c**. The only temperature coefficient for the NH of Arg^5 was small, but NOE was not observed between the D-Tyr^3 C$^\alpha$H and the Arg^5 NH in both **37a** and **37c**. Thus, no hydrogen bond restraints were used in the simulated annealing calculations.

Calculation of Structures. The structure calculations were performed on a Silicon Graphics Origin 2000 workstation with the NMR refine program within the Insight II/Discover package using the consistent valence force field (CVFF).[51] Pseudoatoms were defined for the methylene protons of Nal^1, D-Tyr^3, Arg^4, and Arg^5, prochiralities of which were not identified by ^1H NMR data. The restraints, in which the Gly^2 α-methylene participated, were defined for the separate protons without definition of the prochiralities. The dihedral ϕ angle constraints were calculated based on the Karplus equation: $^3J(H^N,H^\alpha) = 6.7 \cos^2(\theta - 60°) - 1.3 \cos(\theta - 60°) + 1.5$.[52] Lower and upper angle errors were set to 15°. The NOESY spectrum with a mixing time of 400 ms was used for the estimation of the distance restraints between protons. The NOE intensities were classified into three categories (strong, medium, and weak) based on the number of contour lines in the cross peaks to define the upper-limit distance restraints (2.7, 3.5, and 5.0 Å, respectively). The upper-limit restraints were increased by 1.0 Å for the involved pseudoatoms. Lower bounds between nonbonded atoms were set to their van der Waals radii (1.8 Å). These distance and dihedral angle restraints were included with force constants of 25–100 kcal/mol·Å^2 and 25–100 kcal/mol·rad^2, respectively. The 50 initial structures generated by the NMR refine program randomly were subjected to the simulated annealing calculations. The final minimization stage was achieved until the maximum derivative became less than 0.01 kcal/mol·Å^2 by the steepest descents and conjugate gradients methods.

grateful for a Research Fellowship from the Japan Society for the Promotion of Science for Young Scientists.

References

(1) Kaltenbronn, J. S.; Hudspeth, J. P.; Lunney, E. A.; Michniewicz, B. M.; Nicolaides, E. D.; Repine, J. T.; Roark, W. H.; Stier, M. A.; Tinney, F. J.; Woo, P. K. W.; Essenburg, A. D. Renin inhibitors containing isosteric replacements of the amide bond connecting the P$_3$ and P$_2$ sites. *J. Med. Chem.* **1990,** *33,* 838–845.

(2) Ibuka, T.; Habashita, H.; Otaka, A.; Fujii, N. A highly stereoselective synthesis of (*E*)-alkene dipeptide isosteres via organocyanocopper–lewis acid mediated reaction. *J. Org. Chem.* **1991,** *56,* 4370–4382.

(3) Wipf, P.; Fritch, P. C. S$_N$2′ reactions of peptide aziridines. A cuprate-based approach to (*E*)-alkene isosteres. *J. Org. Chem.* **1994,** *59,* 4875–4886.

(4) Fujii, N.; Nakai, K.; Tamamura, H.; Otaka, A.; Mimura, N.; Miwa, Y.; Taga, T.; Yamamoto, Y.; Ibuka, T. S$_N$2′ ring opening of aziridines bearing an α,β-unsaturated ester group with organocopper reagents. A new stereoselective synthetic route to (*E*)-alkene dipeptide isosteres. *J. Chem. Soc., Perkin Trans. 1* **1995,** 1359–1371.

(5) Daly, M. J.; Ward, R. A.; Thompson, D. F.; Procter, G. Allylsilanes in organic synthesis; stereoselective synthesis of *trans*-alkene peptide isosteres. *Tetrahedron Lett.* **1995,** *36,* 7545–7548.

(6) Tamamura, H.; Hiramatsu, K.; Miyamoto, K.; Omagari, A.; Oishi, S.; Nakashima, H.; Yamamoto, N.; Kuroda, Y.; Nakagawa, T.; Otaka, A.; Fujii, N. Synthesis and evaluation of pseudopeptide analogues of a specific CXCR4 inhibitor, T140: The insertion of an (*E*)-alkene dipeptide isostere into the βII′-turn moiety. *Bioorg. Med. Chem. Lett.* **2002,** *12,* 923–928.

(7) Tamamura, H.; Koh, Y.; Ueda, S.; Sasaki, Y.; Yamasaki, T.; Aoki, M.; Maeda, K.; Watai, Y.; Arikuni, H.; Otaka, A.; Mitsuya, H.; Fujii, N. Reduction of peptide character of HIV protease inhibitors that exhibit nanomolar potency against multi-drug resistant HIV-1 strains. *J. Med. Chem.* **2003,** *46,* 1764–1768.

(8) Tamamura, H.; Yamashita, M.; Muramatsu, H.; Ohno, H.; Ibuka, T.; Otaka, A.; Fujii, N. Regiospecific ring-opening reactions of aziridines bearing an α,β-unsaturated ester group with trifluoroacetic acid or methanesulfonic acid: Application to the stereoselective synthesis of (*E*)-alkene dipeptide isosteres. *Chem. Commun.* **1997,** 2327–2328.

(9) Tamamura, H.; Yamashita, M.; Nakajima, Y.; Sakano, K.; Otaka, A.; Ohno, H.; Ibuka, T.; Fujii, N. Regiospecific ring-opening reactions of β-aziridinyl α,β-enoates with acids: application to the stereoselective synthesis of a couple of diastereoisomeric (*E*)-alkene dipeptide isosteres from a single β-aziridinyl α,β-enoate and to the convenient preparation of amino alcohols bearing α,β-unsaturated ester groups. *J. Chem. Soc., Perkin Trans. 1,* **1999,** 2983–2996.

(10) Oishi, S.; Tamamura, H.; Yamashita, M.; Odagaki, Y.; Hamanaka, N.; Otaka, A.; Fujii, N. Stereoselective synthesis of a set of two functionalized (*E*)-alkene dipeptide isosteres of L-amino acid-L-Glu and L-amino acid-D-Glu. *J. Chem. Soc., Perkin Trans. 1* **2001,** 2445–2451.

(11) Nakamura, E.; Aoki, S.; Sekiya, K.; Oshino, H.; Kuwajima, I. Carbon–carbon bond-forming reactions of zinc homoenolate of esters. A novel three-carbon nucleophile with general synthetic utility. *J. Am. Chem. Soc.* **1987,** *109,* 8056–8066.

(12) Ochiai, H.; Tamaru, Y.; Tsubaki, K.; Yoshida, Z. Unsaturated ester synthesis via copper(I)-catalyzed allylation of zinc esters. *J. Org. Chem.* **1987,** *52,* 4418–4420.

(13) Yeh, M. C. P.; Knochel, P. 2-Cyanoethylzinc iodide: A new reagent with reactivity umpolung.*Tetrahedron Lett.* **1988,** *29,* 2395–2396.

(14) Knochel, P.; Yeh, M. C. P.; Berk, S. C.; Talbert, J. Synthesis and reactivity toward acyl chlorides and enones of the new highly functionalized copper reagents RCu(CN)ZnI. *J. Org. Chem.* **1988,** *53,* 2390–2392.

(15) Zhu, L.; Wehmeyer, R. M.; Rieke, R. D. The direct formation of functionalized alkyl(aryl)zinc halides by oxidative addition of highly reactive zinc with organic halides and their reactions with

acid chlorides, α,β-unsaturated ketones, and allylic, aryl, and vinyl halides. *J. Org. Chem.* **1991,** *56,* 1445–1453.

(16) Fujii, N.; Oishi, S.; Hiramatsu, K.; Araki, T.; Ueda, S.; Tamamura, H.; Otaka, A.; Kusano, S.; Terakubo, S.; Nakashima, H.; Broach, J. A.; Trent, J. O.; Wang, Z.; Peiper, S. C. Molecular-size reduction of a potent CXCR4–chemokine antagonist using orthogonal combination of conformation- and sequence-based libraries. *Angew. Chem., Int. Ed.* **2003,** *42,* 3251–3253.

(17) Koshiba, T.; Hosotani, R.; Miyamoto, Y.; Ida, J.; Tsuji, S.; Nakajima, S.; Kawaguchi, M.; Kobayashi, H.; Doi, R.; Hori, T.; Fujii, N.; Imamura, M. Expression of stromal cell-derived factor 1 and CXCR4 ligand receptor system in pancreatic cancer: a possible role for tumor progression. *Clin. Cancer. Res.* **2000,** *6,* 3530–3535.

(18) Müller, A.; Homey, B.; Soto, H.; Ge, N.; Catron, D.; Buchanan, M. E.; McClanahan, T.; Murphy, E.; Yuan, W.; Wagner, S. N.; Barrera, J. L.; Mohar, A.; Verastegui, E.; Zlotnik, A. Involvement of chemokine receptors in breast cancer metastasis. *Nature* **2001,** *410,* 50–56.

(19) Tamamura, H.; Hori, A.; Kanzaki, N.; Hiramatsu, K.; Mizumoto, M.; Nakashima, H.; Yamamoto, N.; Otaka, A.; Fujii, N. T140 analogs as CXCR4 antagonists identified as anti-metastatic agents in the treatment of breast cancer. *FEBS Lett.* **2003,** *550,* 79–83.

(20) Feng, Y.; Broder, C. C.; Kennedy, P. E.; Berger, E. A. HIV-1 entry co-factor: Functional cDNA cloning of a seven-transmembrane, G protein-coupled receptor. *Science* **1996,** *272,* 872–877.

(21) Nanki, T.; Hayashida, K.; El-Gabalawy, H. S.; Suson, S.; Shi, K.; Girschick, H. J.; Yavuz, S.; Lipsky, P. E. Stromal cell-derived factor-1-CXC chemokine receptor interactions play a central role in CD4$^+$ T cell accumulation in rheumatoid arthritis synovium. *J. Immunol.* **2000,** *165,* 6590–6598.

(22) Tamamura, H.; Fujisawa, M.; Hiramatsu, K.; Mizumoto, M.; Nakashima, H.; Yamamoto, N.; Otaka, A.; Fujii, N. Identification of a CXCR4 antagonist, a T140 analog, as an anti-rheumatoid arthritis agent. *FEBS Lett.* **2004,** *569,* 99–104.

(23) Tamamura, H.; Nakajima, T.; Koyanagi, Y.; Tachibana, K.; Fujii, N.; Tamamura, H.; Yoshida, N.; Waki, M.; Matsumoto, A.; Yoshie, O.; Kishimoto, T.; Yamamoto, N.; Nagasawa, T. A small molecule CXCR4 inhibitor that blocks T cell line-tropic HIV-1 infection. *J. Exp. Med.,* **1997,** *186,* 1389–1393.

(24) Schols, D.; Struyf, S.; Van Damme, J.; Este, J. A.; Henson, G.; De Clercq, E. Inhibition of T-tropic HIV strains by selective antagonization of the chemokine receptor CXCR4. *J. Exp. Med.* **1997,** *186,* 1383–1388.

(25) Donzella, G. A.; Schols, D.; Lin, S. W.; Este J. A.; Nagashima, K. A.; Maddon, P. J.; Allaway, G. P.; Sakmar, T. P.; Henson, G.; De Clercq, E.; Moore, J. P. AMD3100, a small molecule inhibitor of HIV-1 entry via the CXCR4 co-receptor. *Nat. Med.* **1998,** *4,* 72–77.

(26) Doranz, B. J.; Grovit-Ferbas, K.; Sharron, M. P.; Mao, S.-H.; Bidwell Goetz, M.; Daar, E. S.; Doms, R. W.; O'Brien, W. A. A small-molecule inhibitor directed against the chemokine receptor CXCR4 prevents its use as an HIV-1 coreceptor. *J. Exp. Med.* **1997,** *186,* 1395–1400.

(27) Howard, O. M. Z.; Oppenheim, J. J.; Hollingshead, M. G.; Covey, J. M.; Bigelow, J.; McCormack, J. J.; Buckheit, Jr., R. W.; Clanton, D. J.; Turpin, J. A.; Rice, W. G. Inhibition of in vitro and in vivo HIV replication by a distamycin analogue that interferes with chemokine receptor function: a candidate for chemotherapeutic and microbicidal application. *J. Med. Chem.* **1998,** *41,* 2184–2193.

(28) Tamamura, H.; Xu, Y.; Hattori, T.; Zhang, X.; Arakaki, R.; Kanbara, K.; Omagari, A.; Otaka, A.; Ibuka, T.; Yamamoto, N.; Nakashima, H.; Fujii, N. A low molecular weight inhibitor against the chemokine receptor CXCR4: a strong anti-HIV peptide T140. *Biochem. Biophys. Res. Commun.* **1998,** *253,* 877–882.

(29) Tamamura, H.; Omagari, A.; Oishi, S.; Kanamoto, T.; Yamamoto, N.; Peiper, S. C.; Nakashima, H.; Otaka, A.; Fujii, N. Pharmacophore identification of a specific CXCR4 inhibitor, T140, leads to development of effective anti-HIV agents with very high selectivity indexes. *Bioorg. Med. Chem. Lett.* **2000,** *10,* 2633–2637.

(30) Fujii, N.; Nakashima, H.; Tamamura, H. The therapeutic potential of CXCR4 antagonists in the treatment of HIV. *Expert Opin. Invest. Drugs* **2003,** *12,* 185–195.

(31) Fukami, T.; Nagase, T.; Fujita, K.; Hayama, T.; Niiyama, K.; Mase, T.; Nakajima, S.; Fukuroda, T.; Saeki, T.; Nishikibe, M.; Ihara, M.; Yano, M.; Ishikawa, K. Structure–activity relationships of cyclic pentapeptide endothelin A receptor antagonists. *J. Med. Chem.* **1995,** *38,* 4309–4324.

(32) Haubner, R.; Gratias, R.; Diefenbach, B.; Goodman, S. L.; Jonczyk, A.; Kessler, H. Structural and functional aspects of RGD-containing cyclic pentapeptides as highly potent and selective integrin αVβ3 antagonists. *J. Am. Chem. Soc.* **1996,** *118,* 7461–7472.

(33) Spatola, A. F.; Crozet, Y.; deWit, D.; Yanagisawa, M. Rediscovering an endothelin antagonist (BQ-123): A self-deconvoluting cyclic pentapeptide library. *J. Med. Chem.* **1996**, *39*, 3842–3846.

(34) Wermuth, J.; Goodman, S. L.; Jonczyk, A.; Kessler, H. Stereoisomerism and biological activity of the selective and superactive αVβ3 integrin inhibitor cyclo(--RGDfV-) and its retro-inverso peptide. *J. Am. Chem. Soc.* **1997**, *119*, 1328–1335.

(35) Haubner, R.; Finsinger, D.; Kessler, H. Stereoisomeric peptide libraries and peptidomimetics for designing selective inhibitors of the αVβ3 integrin for a new cancer therapy. *Angew. Chem., Int. Ed. Engl.* **1997**, *36*, 1374–1389.

(36) Porcelli, M.; Casu, M.; Lai, A.; Saba, G.; Pinori, M.; Cappelletti, S.; Mascagni, P. Cyclic pentapeptides of chiral sequence DLDDL as scaffold for antagonism of G-protein coupled receptors: Synthesis, activity and conformational analysis by NMR and molecular dynamics of ITF 1565 a substance P inhibitor. *Biopolymers* **1999**, *50*, 211–219.

(37) Oishi, S.; Kamano, T.; Niida, A.; Odagaki, Y.; Hamanaka, N.; Yamamoto, M.; Ajito, K.; Tamamura, H.; Otaka, A.; Fujii, N. Diastereoselective synthesis of new ψ[(E)-CH=CMe]- and ψ[(Z)-CH=CMe]-type alkene dipeptide isosteres by organocopper reagents and application to conformationally restricted cyclic RGD peptidomimetics. *J. Org. Chem.* **2002**, *67*, 6162–6173.

(38) Tamamura, H.; Hiramatsu, K.; Kusano, S.; Terakubo, S.; Yamamoto, N.; Trent, J. O.; Wang, Z.; Peiper, S. C.; Nakashima, H.; Otaka, A.; Fujii, N. Synthesis of potent CXCR4 inhibitors possessing low cytotoxicity and improved biostability based on T140 derivatives. *Org. Biomol. Chem.* **2003**, *1*, 3656–3662.

(39) Tamamura, H.; Hiramatsu, K.; Mizumoto, M.; Ueda, S.; Kusano, S.; Terakubo, S.; Akamatsu, M.; Yamamoto, N.; Trent, J. O.; Wang, Z.; Peiper, S. C.; Nakashima, H.; Otaka, A.; Fujii, N. Enhancement of the T140-based pharmacophores leads to the development of more potent and bio-stable CXCR4 antagonists. *Org. Biomol. Chem.* **2003**, *1*, 3663–3669.

(40) Inagawa, J.; Ishikawa, M.; Yamaguchi, M. A mild and convenient method for the reduction of organic halides by using a SmI₂-THF solution in the presence of hexamethylphosphoric triamide (HMPA). *Chem. Lett.* **1987**, 1485–1486.

(41) Otaka, A.; Yukimasa, A.; Watanabe, J.; Sasaki, Y.; Oishi, S.; Tamamura, H.; Fujii, N. Application of samarium diiodide (SmI₂)-induced reduction of γ-acetoxy-α,β-enoates with α-specific kinetic electrophilic trapping for the synthesis of amino acid derivatives. *Chem. Commun.* **2003**, 1834–1835.

(42) Fukuyama, T.; Jow, C. K.; Cheng, M. 2- and 4-nitrobenzenesulfonamides: exceptionally versatile means for preparation of secondary amines and protection of amines. *Tetrahedron Lett.* **1995**, *36*, 6373–6374.

(43) Maligres, P. E.; See, M. M.; Askin, D.; Reider, P. J. Nosylaziridines: activated aziridine electrophiles. *Tetrahedron Lett.* **1997**, *38*, 5253–5256.

(44) Mitsunobu, O. The use of diethyl azodicarboxylate and triphenylphosphine in synthesis and transformation of natural products. *Synthesis* **1981**, *1*, 1–28.

(45) Blanchette, M. A.; Choy, W.; Davis, J. T.; Essenfeld, A. P.; Masamune, S.; Roush, R. W.; Sakai, T. Horner-Wadsworth-Emmons reaction: Use of lithium chloride and an amine for base-sensitive compounds. *Tetrahedron Lett.* **1984**, *25*, 2183–2186.

(46) Abdel-Magid, A. F.; Maryanoff, C. A.; Carson, K. G. Reductive amination of aldehydes and ketones by using sodium triacetoxyborohydride. *Tetrahedron Lett.* **1990**, *31*, 5595–5598.

(47) Honzl, J.; Rudinger, J. Amino acids and peptides. XXXIII. Nitrosyl chloride and butyl nitrite as reagents in peptide synthesis by the azide method; suppression of amide formation. *Collect. Czech. Chem. Commun.* **1961**, *26*, 2333–2344.

(48) Nakashima, H.; Masuda, M.; Murakami, T.; Koyanagi, Y.; Matsumoto, A.; Fujii, N.; Yamamoto, N. Anti-human immunodeficiency virus activity of a novel synthetic peptide, T22 ([Tyr-5, 12, Lys-7]polyphemusin II): a possible inhibitor of virus-cell fusion. *Antimicrob. Agents Chemother.* **1992**, *36*, 1249–1255.

(49) Navenot, J. M.; Wang, Z. X.; Trent, J. O.; Murray, J. L.; Hu, Q. X.; DeLeeuw, L.; Moore, P. S.; Chang, Y.; Peiper, S. C. Molecular anatomy of CCR5 engagement by physiologic and viral chemokines and HIV-1 envelope glycoproteins: Differences in primary structural requirements for RANTES, MIP-1α, and vMIP-II binding. *J. Mol. Biol.* **2001**, *313*, 1181–1193.

(50) Intramolecular hydrogen bonds were not observed in the calculated structure. Thus, the EADI-containing pseudopeptides, which are discussed in this study, do not seem to exist in a characteristic turn conformation such as a βII'γ turn as reported in several papers concerning normal cyclic pentapeptides, see Nikiforovich, G. V.; Kover, K. E.; Zhang, W.-J.; Marshall, G. R. Cyclopentapeptides as flexible conformational templates. *J. Am. Chem. Soc.* **2000**, *122*, 3262–3273.

(51) Miyamoto, K.; Nakagawa, T.; Kuroda, Y. Solution structure of the cytoplasmic linker between domain III–S6 and domain IV–S1 (III–IV linker) of the rat brain sodium channel in SDS micelles. *Biopolymers* **2001**, *59*, 380–393.

(52) Ludvigsen, S.; Andersen, K. V.; Poulsen, F. M. Accurate measurements of coupling-constants from 2-dimensional nuclear-magnetic-resonance spectra of proteins and determination of φ-angles *J. Mol. Biol.* **1991**, *217*, 731–736.

JM049429H

Bioluminescence Resonance Energy Transfer Reveals Ligand-induced Conformational Changes in CXCR4 Homo- and Heterodimers*

Yann Percherancier‡§, Yamina A. Berchiche‡¶, Isabelle Slight‡¶, Rudolf Volkmer-Engert‖, Hirokazu Tamamura**, Nobutaka Fujii**, Michel Bouvier‡§§, and Nikolaus Heveker‡¶‡‡

From the ‡Department of Biochemistry, Université de Montréal, Montréal H3C 3J7, Québec, Canada, the ¶Research Centre/Hôpital Sainte-Justine, Montréal, Québec, H3T 1C5, Canada, the ‖Institute for Medical Immunology, Department of Molecular Libraries, Charité-Universitätsmedizin, 10117 Berlin, Germany, and **Graduate School of Pharmaceutical Sciences, Kyoto University, Kyoto 606-8501, Japan

Homo- and heterodimerization have emerged as prominent features of G-protein-coupled receptors with possible impact on the regulation of their activity. Using a sensitive bioluminescence resonance energy transfer system, we investigated the formation of CXCR4 and CCR2 chemokine receptor dimers. We found that both receptors exist as constitutive homo- and heterodimers and that ligands induce conformational changes within the pre-formed dimers without promoting receptor dimer formation or disassembly. Ligands with different intrinsic efficacies yielded distinct bioluminescence resonance energy transfer modulations, indicating the stabilization of distinct receptor conformations. We also found that peptides derived from the transmembrane domains of CXCR4 inhibited activation of this receptor by blocking the ligand-induced conformational transitions of the dimer. Taken together, our data support a model in which chemokine receptor homo- and heterodimers form spontaneously and respond to ligand binding as units that undergo conformational changes involving both protomers even when only one of the two ligand binding sites is occupied.

In recent years, the concept of GPCR[1] dimerization has raised questions about the molecular details and functional role of such oligomeric assembly (for a recent review, see Ref.

[1] The abbreviations used are: GPCR, G-protein-coupled receptor; RET, resonance energy transfer; BRET, bioluminescence resonance energy transfer; HEK, human embryonic kidney; PBS, phosphate-buffered saline; YFP, yellow fluorescent protein; RLuc, Renilla luciferase; BSA, bovine serum albumin; $BRET_{50}$, 50% of the maximal BRET signal; HIV, human immunodeficiency virus; TM, transmembrane.

1). Given the clinical interest in GPCRs, insights into the structural and functional organization of the receptor complexes have the potential to facilitate the design of new drug candidates with increased efficacy and selectivity. Resonance energy transfer (RET) techniques have emerged as methods of choice to study receptor dimerization in living cells. Although most RET studies indicate that many if not all GPCRs exist as dimers or higher oligomers under basal conditions, apparent contradictions exist concerning their potential dynamic regulation upon ligand binding. Although numerous authors did not find any effects of ligands on constitutive RET signals in their systems (2–8), others observed ligand-promoted increases or decreases that were interpreted as either the formation (9–11) or the dissociation (12–15) of GPCR dimers in response to receptor activation. Conformational changes within pre-existing constitutive dimers have also been proposed as alternative explanations for agonist or antagonist-induced changes in RET (16–18).

Chemokine receptors such as CCR2 and CXCR4 have been reported to form homo- and heterodimers (3, 4, 19–24). In early co-immunoprecipitation studies, Vila-Coro et al. (21) proposed that the dimerization of CXCR4 is induced upon activation by its chemokine ligand SDF-1. In contrast, data obtained with RET techniques revealed that CXCR4 homo-dimers form spontaneously in the absence of ligand (3, 4, 24). In one study, no significant effect of SDF-1 was observed on the constitutive energy transfer (4), whereas a small but reproducible increase was detected by others (24). As for CXCR4, agonist stimulation of CCR2 was found to promote the formation of dimers as revealed by chemical cross-linking followed by immunoprecipitation, suggesting that receptor dimerization and activation are interconnected processes (19). Heterodimerization between CXCR4 and CCR2 has initially been proposed to occur only in the case of a frequent genetic variant of CCR2, termed CCR2V64I, but not for the wild-type form of CCR2 (20). Given that CCR2V64I was associated with delayed AIDS progression (25–27), such a specific heterodimerization pattern could have important pathophysiological consequences. Indeed, it has been speculated that the AIDS-protective phenotype of the variant could be the result of its block of HIV entry via CXCR4 (20). In line with this proposition, the same authors proposed that the antiviral properties of a monoclonal anti-CCR2 antibody resulted from its ability to force the heterodimerization of CCR2 with CXCR4 (23).

Taken together, the results summarized above raise a number of questions concerning the dynamic nature of the homo- and heterodimerization processes regulating GPCR function.

−190−

Among these, the question of whether receptor ligands can induce homo- or heterodimer association or dissociation or promote conformational changes within preformed dimers that remain stable through the activation cycle is still highly debated. The potential role of CXCR4/CCR2 heterodimerization in inhibiting HIV entry makes it a particularly relevant model to study this question. In addition to their role in HIV infection, these chemokine receptors have been shown to be involved in cancer metastasis as well as in various aspects of inflammatory diseases including the directed migration of leukocytes during acute immune responses and homing (28–34). Therefore, understanding the dynamics of CXCR4/CCR2 homo- and heterodimerization after ligand binding takes on a particular importance when considering their potential as drug targets for numerous disease states.

In the present study, we took advantage of bioluminescence resonance energy transfer (BRET) approaches to study CXCR4/CCR2 homo- and heterodimers in the course of receptor activation. We found that CXCR4 and CCR2 exist as constitutive homo- and heterodimers and that different ligands promote distinct conformational rearrangements of preformed stable oligomers. Our data also indicate that peptides derived from CXCR4 transmembrane domains block receptor activation by preventing the agonist-promoted conformational rearrangement of both CXCR4 homo- and CXCR4/CCR2 heterodimers.

EXPERIMENTAL PROCEDURES

Plasmids—The cloning of CXCR4-YFP and CXCR4-RLuc have been described previously (3). CCR2-YFP and CCR2-RLuc were constructed by ligating the coding sequence of CCR2, after its amplification by PCR, into the pGFP-N1-Topaze (PerkinElmer Life and Analytical Sciences) and (hRLuc)-N3 (BioSignal) backbones of the CXCR4-YFP and -RLuc using the HinDIII and AgeI or HinDIII and BamHI sites, respectively. The constructs were sequenced to ensure the absence of unwanted mutations. The 64V and 64I variants were obtained by site-directed mutagenesis using the Kunkel method. The amino acid sequence of the fusion linker regions between the terminal receptor residue and the initiator methionine of either YFP or RLuc were as follows: CXCR4-YFP, FHSS*KPVAT*MVSKG; CXCR4-RLuc, FHSS*KPGDPPARAT*-MTSKV; CCR2-YFP, SAGL*GPVAT*MVSKG; and CCR2-RLuc, SAGL-*GDPPARAT*MTSKV. Bold italic characters identify linker residues resulting from the cloning strategy and that derive neither from the receptor nor the fluorophore sequences. The sequences of the linker regions and of the mutated residues were verified by direct sequencing.

Reagents—SDF-1 and MCP-1 were purchased from PeproTech and AMD3100 was obtained from the NIH AIDS Research & Reference Reagent Program. TC14012, a T140 analogue with similar biological properties, was synthesized as described previously (35). The sequences of the CXCR4 transmembrane domain-derived peptides as described in Tarasova *et al.* (36) were synthesized using Fmoc (*N*-(9-fluorenyl)methoxycarbonyl) solid phase synthesis as described previously (37), purified to >95% purity and characterized by matrix-assisted laser desorption ionization/time of flight mass spectrometry. The sequences of the peptides are as follows: CXCR4-TMII, LLFVITLPFWAVDAVANWYFGN-DD-OH; CXCR4-TMIV, VYVGVWIPALLLTIPDFIFANDD-OH; CXCR-4-TMVI, VILILAFFACWLPYYIGISID-OH; CXCR4-TMVII, DDEALA-FFHCCLNPILYAFL-NH₂. β2AR-TMVI-1 (NH₂-GIIMGTFTLCWLPFF-IVNIVH-COOH) and β2AR-TMVI-2 (NH₂-AIIMATFTACWLPFFIVNI-VH-COOH) were described in Ref. 38. They were dissolved as 10 mM stocks in Me₂SO and used freshly diluted at the concentrations indicated in the text and in the figure legends.

Cell Culture and Transfection—HEK293T cells were maintained in Dulbecco's modified Eagle's medium supplemented with 10% fetal bovine serum, 100 units/ml penicillin and streptomycin, 2 mM L-glutamine (all from Wisent). 24 h before transfection, cells were seeded at a density of 500,000 cells per well in 6-well dishes. Transient transfections were performed using the FuGENE-6 transfection reagent (Roche) in OptiMEM medium (Invitrogen) In general, 0.1 μg of CXCR4-RLuc or CCR2-RLuc was transfected alone or with increasing quantities of YFP-tagged CXCR4 or CCR2. The total amount of DNA transfected in each well was completed to 2 μg with empty vector. After overnight incubation, transfection medium was replaced with fresh Dulbecco's modified Eagle's medium for 3 h to allow cell recovery. Transfected cells were then seeded in 96-well white plates (with clear bottoms that had

been pre-treated with poly-D-lysine) and left in culture for 24 h before being processed for BRET assay.

Flow Cytometry—Transfected HEK293T cells were detached with phosphate-buffered saline (PBS) containing 1 mM EDTA 24 h after cotransfection with CXCR4-RLUC and CXCR4-YFP as indicated. Peripheral blood mononuclear cells (PBMC) were isolated on a Ficoll (Amersham Biosciences) gradient from whole blood. The cells were stimulated with 10 μg/ml phytohemagglutinin and cultured for 7 days in RPMI containing 10% fetal bovine serum and 50 IU/ml interleukin-2. For CXCR4 staining, the cells were incubated 45 min at 4 °C in PBS containing 2% fetal bovine serum with anti-CXCR4 phycoerythrin-conjugated 12G5 monoclonal antibody (Santa Cruz Biotechnology). They were then washed three times with PBS, and cell surface expression of CXCR4 was quantified by flow cytometry on a FACSCalibur flow cytometer (BD Biosciences).

BRET Assays—For routine BRET measurements, cells were washed once with PBS 36 to 48 h after transfection and coelenterazine H (Nanolight Technology) added to a final concentration of 5 μM in PBS. Readings were then collected using a multidetector plate reader MITHRAS LB940 (Berthold Technologies, Bad Wildbad, Germany) allowing the sequential integration of the signals detected in the 480 ± 20 nm and 530 ± 20 nm windows for luciferase and YFP light emissions respectively. The BRET signal is determined by calculating the ratio of the light intensity emitted by the Receptor-YFP over the light intensity emitted by the Receptor-RLuc. The values were corrected by subtracting the background BRET signal detected when the Receptor-RLuc construct was expressed alone. To assess the effects of ligands, SDF-1, AMD3100, TC14012, and MCP-1 were added at the concentrations indicated in the text and in the figure legends and incubated at 37 °C for 5 min before the addition of coelenterazine H and BRET reading. When indicated, ligands were added in presence of 0.1% BSA (Sigma). For experiments with transmembrane peptides, the cells were pre-incubated with the different peptides in PBS for 15 min at 37 °C before agonist exposure.

For acquisition of full BRET spectra, cells were transfected as described above with different amounts of CXCR4-YFP for a given quantity of CXCR4-RLuc (0.1 μg). Cells were detached and resuspended in PBS containing 0.1% (w/v) glucose. 200,000 cells were seeded in 100 μl of PBS in a 96-well plate with a clear bottom (Corning), and BRET scan was performed in a Flex-station 2 (Molecular Devices) by reading luminescence between 400 and 600 nm immediately after the addition of coelenterazine for cells expressing different [acceptor]/[donor] ratios.

For BRET titration experiments, net BRET ratios were expressed as a function of the [acceptor]/[donor] ratio (39). Total fluorescence and luminescence were used as relative measures of total expression of the acceptor and donor proteins, respectively. Total fluorescence was determined with MITHRAS using an excitation filter at 485 nm and an emission filter at 535 nm. Total luminescence was measured in the MITHRAS, 10 min after the addition of coelenterazine and the reading taken in the absence of emission filter.

cAMP Production—To determine cAMP accumulation, HEK293T cells were seeded in 24-well microplates at 10⁵ cells/well (coated with 0.1% poly-D-lysine) 24 h before the experiment and labeled for 2–3 h in Dulbecco's modified Eagle's medium without fetal bovine serum containing 2 μCi/ml [³H]adenine (PerkinElmer Life and Analytical Sciences). Because CXCR4 is coupled to Gi proteins, the relative efficacy of SDF-1 to inhibit forskolin-induced cAMP production was monitored in different conditions. Cells were stimulated in presence of 20 μM forskolin (Sigma) alone or 20 μM forskolin and 1 nM SDF-1 for 30 min at 37 °C in Dulbecco's modified Eagle's medium containing 50 mM HEPES, pH 7.4, 0.1% BSA, 1 mM 3-isobutyl-1-methylxanthine (Sigma) and supplemented or not with 10 μM of each of the CXCR4 TM peptides. The reaction was terminated by removing the Dulbecco's modified Eagle's medium/3-isobutyl-1-methylxanthine/ligand solution and the addition of ice-cold 5% trichloroacetic acid. [³H]cAMP was purified by sequential chromatography (Dowex resin/aluminum oxide).

Binding Assays—SDF-1 binding to CXCR4 was assessed indirectly by flow cytometry as described previously (40). In brief, the ability of SDF-1 to compete for the binding of the monoclonal anti-CXCR4 antibody 12G5 to CEM cells was used to determine SDF-1 binding. SDF-1 was co-incubated at 4 °C for 30 min with the antibody and SDF binding determined by the loss of 12G5 labeling, as determined by flow cytometry. To test whether CXCR4 TM peptides interfered with SDF-1 binding to CXCR4, the peptides were incubated with the cells 15 min before addition of SDF-1 and 12G5. Control tubes were incubated with peptides and 12G5, without SDF-1.

For T14012 binding assay, CXCR4-expressing HEK293T cells were detached with 5 mM EDTA, washed twice in binding buffer (50 mmol/L
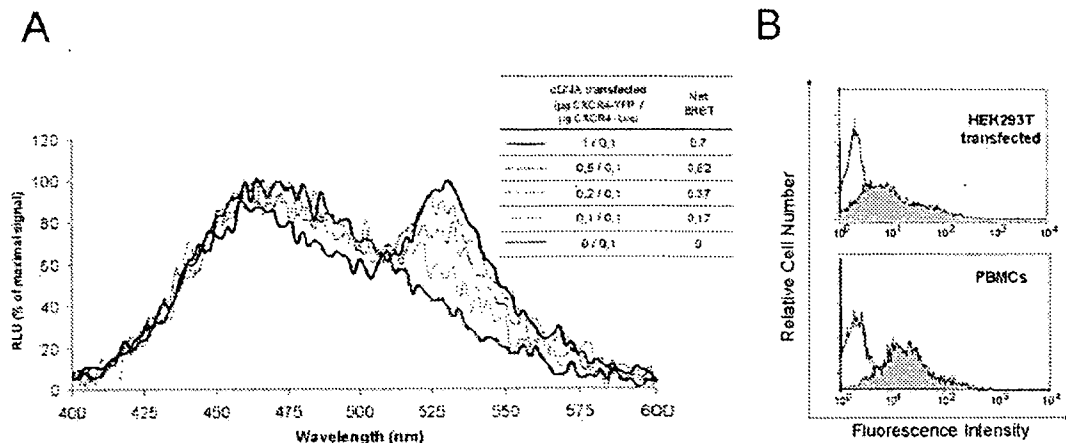
A

B

FIG. 1. *A*, light emission BRET spectra for CXCR4 homodimerization. Spectra of HEK293T cells coexpressing a fix amount of BRET donor (CXCR4-RLuc) and various levels of acceptor (CXCR4-YFP). Net BRET signals and BRET spectra were determined in parallel. Results are expressed as percentage of the maximum signal obtained when CXCR4-RLuc is transfected alone. *B*, CXCR4 expression of transfected and primary cells: relative CXCR4 expression in transiently transfected HEK293T cells (0.1 μg of CXCR4-Luc and 1 μg of CXCR4-YFP) and in activated peripheral mononuclear blood cells *(PBMCs)* by flow cytometry using the anti-CXCR4-PE antibody.

HEPES, pH 7.4, 1 mmol/L $CaCl_2$, 5 mmol/L $MgCl_2$, and 0.5% BSA) and resuspended at final concentration of 5 × 10^5 cells/ml. Total SDF-1 binding was measured with 0.1 nM ^{125}I-SDF-1 (2200 Ci/mmol; PerkinElmer Life and Analytical Sciences) as tracer, and TC14012 competition assays were performed with 100 nM TC14012 in the presence or absence of 10 μM of each CXCR4 peptide. The samples were incubated for 90 min at 20 °C, and binding was terminated by rapid filtration through glass fiber (GF/C) filters (Whatman) using ice-cold PBS containing 0.5 M NaCl. The retained radioactivity was counted in a γ counter (1271 RIAgamma Counter; PerkinElmer Life and Analytical Sciences).

Data Analysis—Data obtained in BRET assays were analyzed using Prism 3.0. Statistical significance of the differences between the different conditions were calculated using one-way analysis of variance with a Bonferroni post-test for *p* values less than 0.05.

RESULTS

Constitutive CXCR4 Dimers Revealed by BRET—The existence of constitutive CXCR4 dimers was probed by monitoring the occurrence of intermolecular interactions among CXCR4 molecules under basal conditions using a proximity-based BRET assay. For this purpose, a constant amount of CXCR4-RLuc expression vector was cotransfected with increasing amounts of CXCR4-YFP encoding plasmid. The entire emission spectrum between 400 and 600 nm was then analyzed for various CXCR4-YFP/CXCR4-RLuc (energy acceptor/energy donor) ratios after the addition of the luciferase substrate coelenterazine. As shown in Fig. 1, increasing the expression level of CXCR4-YFP led to a progressive increase in the amount of light emitted in the 510–550 nm region that resulted from the transfer of energy from the luciferase to the YFP with the ensuing emission of light by the latter (Fig. 1A). The occurrence of BRET between RLuc and YFP was further illustrated by the reduction in emission observed in the 450–510 nm part of the spectrum that corresponds to the region of overlap between RLuc (energy donor) emission and YFP (energy acceptor) excitation wavelengths allowing the energy transfer. The basal BRET observed in the absence of any receptor ligand indicates, in agreement with previous reports (3, 4, 24), that CXCR4 exists as a constitutive homodimer. For all subsequent BRET experiments, the emission of light was measured only in the 460–500 nm and 510–550 nm windows, corresponding to the RLuc and YFP emission peaks, respectively, and the BRET defined as the ratio of light detected in these two channels after coelenterazine addition. As can be seen in Fig. 2A, the BRET signal increased as a hyperbolic function of the CXCR4-YFP/CXCR4-RLuc ratio. The saturation of the BRET titration curve

is indicative of a specific protein-protein interaction, because random molecular collisions that would give rise to bystander BRET would be expected to increase nearly linearly over a wide range of YFP/RLuc (39, 41). The selectivity of the observed signal is further supported by the fact that co-expression of CXCR4-RLuc with an unrelated GPCR, GBR2-YFP, led to marginal signal that progressed linearly over the same range of energy acceptor/donor. The positive BRET signal did not result from a non-physiological overexpression of the receptors, because CXCR4 immunostaining followed by flow cytometry analysis revealed that the highest expression levels reached in transfected HEK293T cells (1 μg of CXCR4-YFP + 0.1 μg of CXCR4-RLuc) was still lower than those observed in activated peripheral blood mononuclear cells (Fig. 1B).

Ligand-induced Modulation of the CXCR4 Homodimer BRET Signal—To assess the effect of ligand binding on the BRET signal observed for the CXCR4 homodimer, full BRET titration curves were obtained in the presence and absence of the CXCR4 agonist SDF-1 or the polyphemusin II-derived inverse agonists peptide analogue TC14012 (35). As can be seen in Fig. 2A, the addition of SDF-1 increased the maximal BRET signal observed, whereas TC14012 decreased it. It is interesting that neither compound affected the shape of the curve so that the concentration of CXCR4-YFP needed to reach 50% of the maximal BRET signal ($BRET_{50}$) remained unaffected by the treatments. Because the $BRET_{50}$ represents the propensity of the protomers to interact with one another (*i.e.* their relative affinity), our data indicate that the ligand treatments did not change the number of complexes. Rather, the maximal BRET signal increase most likely reflects conformational changes within preformed receptor dimers, that affect the distance between the energy donor and acceptor. SDF-1 had no effect on the marginal signal observed between CXCR4-RLuc and the unrelated GBR2-YFP, confirming the selectivity of the effect.

The dose dependence of the ligand effect is illustrated in Fig. 2B. In cell expressing a given CXCR4-RLuc/CXCR4-YFP ratio, the agonist SDF-1 and inverse agonist TC14012 dose-dependently increase and decrease the basal BRET signal, respectively. It is interesting that the bicyclam weak partial agonist AMD3100 (42) increases the BRET signal, albeit to lower extent than the full agonist SDF-1. The unrelated CCR2-selective chemokine MCP-1 had no effect on the BRET signal, confirming that ligand interaction with CXCR4 is required to promote BRET changes. The dose-response curves were carried out in
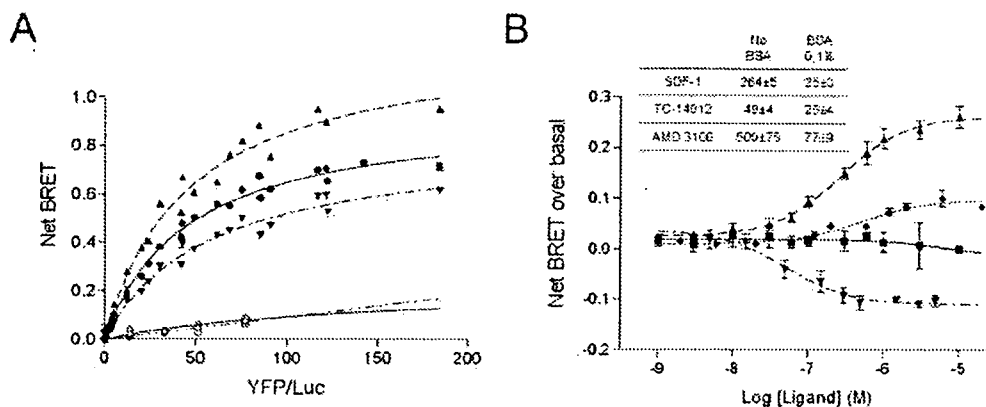
Fig. 2. **Ligand effect on CXCR4 homodimers expressed at physiological levels in HEK293T cells.** HEK293T cells were transiently transfected with 0.1 μg of CXCR4-RLuc and different amounts ranging from 0.03 to 1 μg (*A*) or 1 μg (*B*) of CXCR4-YFP. *A*, saturation curves with and without ligands (700 nM SDF-1 or 500 nM TC14012). Saturation curves were obtained by plotting net BRET as a function of the [Acceptor]/[Donor] ratio (for more detail, see "Experimental Procedures"). As a control of specificity, CXCR4-RLuc BRET was also monitored with increasing quantities of GBR2-YFP in presence (O) or absence (◇) of 700 nM SDF-1. Result represents one experiment of five that gave similar results. BRET$_{50}$ values, measured without ligand or in the presence of SDF-1 or TC14012, were 45.8 ± 3, 46 ± 4.7, and 57.2 ± 5.2, respectively. *B*, dose-response of ligand-induced change in CXCR4/CXCR4 homodimerization BRET. 48 h after transfections, cells were activated for 5 min at 37 °C with increasing concentration of SDF-1, AMD3100, MCP-1, or TC14012 before BRET measurement. The inset compares the nanomolar EC$_{50}$ values found for SDF-1, TC14012, and AMD3100 in the presence or absence of 0.1% BSA used as carrier protein. The results represent the average ± S.E. of four independent experiments done in duplicate. ▲, SDF-1; ▼, TC14012; ◆, AMD3100; ■, MCP-1; ●, no ligand.

both the absence and the presence of the carrier protein BSA (0.1%). As can be seen in the Table inset, the presence of BSA significantly increased the apparent potency of the compounds, indicating the occurrence of nonspecific adsorption or inactivation of the diluted ligands in the absence of carrier. The EC$_{50}$ determined for SDF-1 in the presence of BSA was well within the range of K_d values previously reported for SDF-1 binding to CXCR4 (4–85 nM) (43–47), whereas the EC$_{50}$ for TC14012 and AMD3100 are comparable with the IC$_{50}$ values obtained in binding competition experiments using ^{125}I-SDF-1 as the radioligand (42).

The pharmacological selectivity of the ligand-promoted BRET changes was further demonstrated by the competitive nature of the effects. Indeed, as shown in Fig. 3, TC14012 dose-dependently blocked the ability of 100 nM SDF-1 to increase the BRET signal and eventually reverse this increase revealing the inhibitory action of the inverse agonist (Fig. 3*A*). Likewise, increasing concentration of the partial agonist AMD3100 progressively blocked the SDF-1-promoted BRET increase until it reached the modestly elevated level corresponding to the partial agonistic activity of AMD3100 (Fig. 3*B*). Taken together, these results indicate that three compounds with different intrinsic efficacies led to distinct conformational changes of the CXCR4 dimer.

CCR2 Homo- and Heterodimers—CXCR4 has been previously demonstrated to form heterodimers with CCR2, but it remained unclear whether these heterodimers are spontaneously formed or induced by the presence of one or both receptor ligands (20, 23, 48). To clarify this issue, we first investigated the formation of constitutive CCR2 homodimers and their modulation by the CCR2 selective agonist MCP-1. As can be seen in Fig. 4*A*, saturating hyperbolic BRET titration curves revealed the spontaneous formation of CCR2 homodimer. The selective agonist increased the maximal BRET signal without affecting the BRET$_{50}$ in a manner similar to that observed for the constitutive CXCR4 homodimer, indicating that the conformation and not the number of dimers was affected by the ligand binding. The pharmacological selectivity of the effects was again confirmed by the fact that the CXCR4-selective agonist SDF-1 had no effect on the CCR2 dimer BRET signal (Fig. 4*B*).

As was the case for each of the receptors expressed individually, coexpression of CCR2 and CXCR4 led to the formation of

constitutive heterodimers revealed by specific basal BRET signals and hyperbolic saturating BRET titration curves between CCR2-RLuc and CXCR4-YFP as well as in the reverse orientation (between CXCR4-RLuc and CCR2-YFP) (Fig. 5*A*). It is interesting that the selective binding of ligands to a single protomer was sufficient to promote heterodimer BRET changes for the two BRET orientations. However, the pattern of ligand effects was different from that observed for each of the homodimers. In addition, the BRET pair orientation influenced the ligand response pattern. When considering the CXCR4-RLuc/CCR2-YFP orientation, the addition of the CCR2 agonist MCP-1 led, as was the case for the CCR2 homodimer, to an increase of the heterodimer BRET signal. In contrast, the CXCR4 agonist SDF-1, which promoted an increase of the CXCR4 homodimer BRET, decreased the BRET signal originating from the heterodimer. The CXCR4 inverse agonist TC14012 for its part had a similar effect on the homo- and heterodimer, leading to a decrease in the BRET signal (Fig. 5*B*, *left*). When the reverse BRET partner orientation (CCR2-RLuc/CXCR4-YFP) was investigated, the CXCR4 ligands SDF-1 and TC14012 retained their inhibitory effect on the heterodimer BRET signal. MCP-1, however, which increased the BRET observed between CXCR4-RLuc and CCR2-YFP, led to a dramatic reduction of the BRET signal obtained for the CCR2-RLuc/CXCR4-YFP pair (Fig. 5*B*, *right*). Taken together, these results clearly indicate that the orientation of the ligand-promoted BRET changes cannot be used as a direct reflection of the intrinsic ligand efficacy. Rather, it seems to be dependent on both the nature of the ligand and the BRET pairs considered; both the identity of the receptor protomers and the relative position of the energy donor and acceptor within the dimers influence the responses observed.

The observation that MCP-1 can either increase or decrease the BRET signal emanating from the CXCR4/CCR2 heterodimer depending on the relative RLuc/YFP orientation can hardly be reconciled with the hypothesis that BRET changes reflect ligand-induced dimer association or dissociation. Indeed, the same ligand should not lead to opposite effects on the same receptor heterodimer. Given that both the distance and the orientation between the energy donor and acceptor determine the BRET efficacy, the distinct BRET modulations observed most probably reflect conformational rearrangements

FIG. 3. TC14012 and AMD3100 competition of SDF-1α induced changes in CXCR4 homodimerization BRET signal. HEK293T cells were transfected with 0.1 μg of CXCR4-RLuc and a saturating quantity (1.0 μg) of CXCR4-YFP plasmids. Ligands were added either alone (100 nM SDF-1, 500 nM TC14012, or 2 μM AMD3100), or 100 nM SDF-1 was mixed with increasing quantities of TC14012 or AMD3100. Results are the average of three independent experiments performed in duplicate.
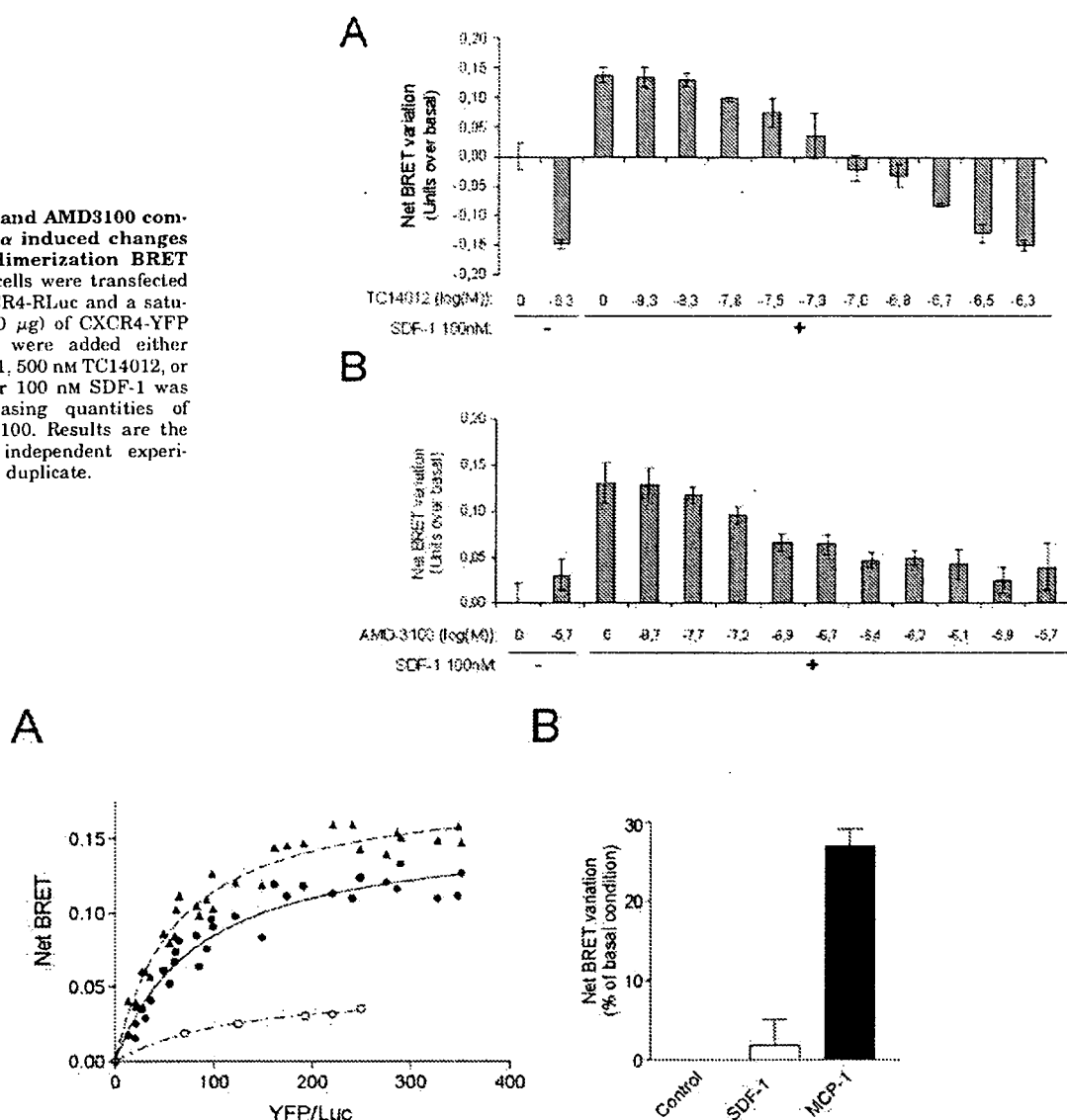
FIG. 4. MCP-1 effect on CCR2 homodimers. A, HEK293T cells were transfected with 0.1 μg of CCR2-RLuc and increasing quantities (from 0.01 to 1.0 μg) of either CCR2-YFP (●, ▲) or GBR2-YFP (O) vectors. Net BRET measured in presence (▲) or absence (●, O) of 200 nM MCP-1 is plotted as a function of the [Acceptor]/[Donor] ratio as in Fig. 2. $BRET_{50}$ values measured for CCR2 homodimer in absence and presence of MCP-1 were 84.2 ± 11.1 and 61.8 ± 5.8, respectively. B, cells transfected with 0.1 μg of CCR2-RLuc and a saturating excess (1.0 μg) of CCR2-YFP plasmids were stimulated with 200 nM MCP-1 or 200 nM SDF-1. Results are the average of three independent experiments performed in triplicate.

that change either the distance or the relative orientation between the fluorophores. Because these parameters are affected by the initial relative position of the RLuc and YFP within the dimers, it is to be expected that the same conformational switch imposed by a ligand could result in very different BRET changes when different BRET configurations are considered.

A previous study suggested that CXCR4/CCR2 heterodimers could be formed only with the CCR2V64I variant form of the receptor and not with the wild-type CCR2 (20). Given that the CCR2 64I variant is associated with delayed AIDS onset in persons infected with HIV, the finding was suggestive that the phenotype of the 64I variant could be mediated by an inhibition of CXCR4 usage by HIV as a result of its heterodimerization (23, 26). To reassess this possibility, we systematically used both CCR2 variants to measure both basal and ligand-modulated BRET signals generated by homo- and heterodimers but failed to detect any significant difference between them (data

not shown). Therefore, the mechanism for the observed protective phenotype against AIDS progression of CCR2V64I is not related to its ability to heterodimerize with CXCR4.

Effects of Peptides Derived from the CXCR4 Transmembrane Domains on both CXCR4 Homo- and Heterodimers—Previous work had found that peptides derived from CXCR4 transmembrane domains are rapidly associating with the receptor, blocking its signaling as well as its HIV-1 coreceptor function (36). We asked whether these effects could result from the dissociation of constitutive CXCR4 dimers, a mechanism that had been suggested for the effect of a peptide derived from TMVI of the β-adrenergic receptor (38). For this purpose, the effect of four peptides derived from TMs II, IV, VI and VII was assessed on the basal CXCR4 homodimer BRET signal. As shown in Fig. 6A, none of the peptides affected the constitutive BRET signal as shown by the unaltered BRET titration curves, ruling out peptide-promoted dissociation as the basis of their functional inhibitory action. However, all peptides blocked the SDF-1-
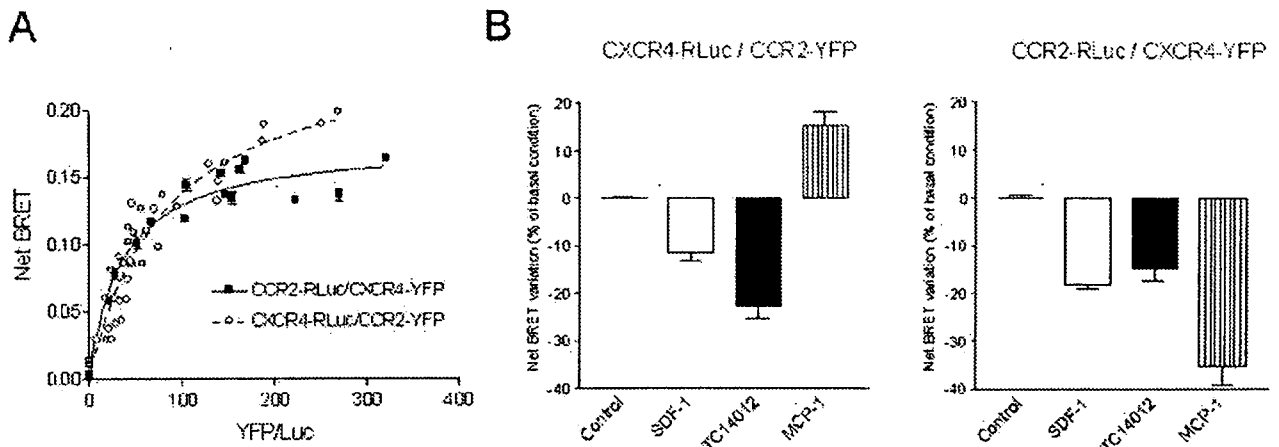
Fig. 5. SDF-1, TC14012, and MCP-1 effects on CXCR4-CCR2 heterodimers. HEK293T cells were transfected with 0.1 μg of either CXCR4-RLuc or CCR2-RLuc and different amounts ranging from 0.03 to 1.0 μg (A) or saturating excess (1.0 μg) (B) of CCR2-YFP or CXCR4-YFP expression vectors. A, CCR2-RLuc/CXCR4-YFP and CXCR4-RLuc/CCR2-YFP saturation curves were obtained by plotting net BRET as a function of the [acceptor]/[donor] ratio as explained in material and methods. B, HEK293T cells transfected either with CXCR4-RLuc/CCR2-YFP (left) or CCR2-RLuc/CXCR4-YFP (right) were stimulated with either 200 nM SDF-1α, 500 nM TC14012, or 200 nM MCP-1 for 5 min at 37 °C before BRET measurement.
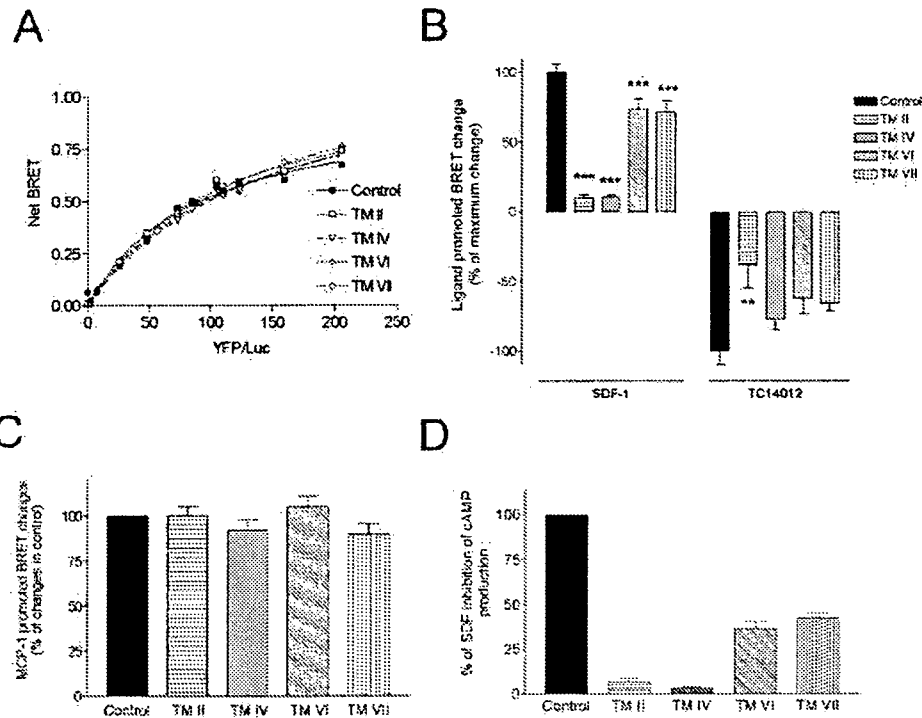

Fig. 6. Effects of CXCR4 TM peptides on CXCR4 homodimers. A, saturation curve of CXCR4 homodimers in the presence or absence of CXCR4 TM peptides. Transiently transfected cells were incubated for 15 min at 37 °C in presence or absence of 10 μM of CXCR4 TMs 2, 4, 6, or 7 before BRET measurement. Longer peptide incubation times (1 h to overnight) yielded identical results (data not shown). B, cells transfected with 0.1 μg of CXCR4-RLuc and saturating excess (1.0 μg) of CXCR4-YFP were incubated with 10 μM of CXCR4 TMII, TMIV, TMVI, or TMVII as in A before being stimulated with 200 nM SDF-1 or 100 nM TC14012. Asterisks indicate significance of the difference between the TM-treated condition and control condition (vehicle alone, black bar). ***, $p < 0.001$; **, $p < 0.01$. Absence of asterisk indicates $p > 0.05$. C, cells transfected with 0.1 μg of CCR2-RLuc and saturating excess (1.0 μg) of CCR2-YFP were left untreated or were treated with 10 μM concentrations of each CXCR4 TM peptide, as in B, but were activated with 200 nM MCP-1. D, HEK293T cells transfected with CXCR4-Luc and CXCR4-YFP were stimulated for 30 min at 37 °C with 20 μM forskolin alone or 20 μM forskolin plus 1 nM SDF-1 in the presence of the vehicle (control) or 10 μM of each CXCR4 TM peptide. The cAMP production was assessed by measuring the accumulation of [³H]cAMP in cells pre-labeled with [³H]adenine and expressed as percentage of the maximal SDF-mediated inhibition in the absence of peptide. Results are expressed as the mean ± S.E. of three to five independent experiments carried out in triplicate.

induced BRET increase, and TMs II and IV were the most efficacious (Fig. 6B), indicating that inhibition of the agonist-promoted conformational change could underlie the mechanism of action of the peptides. It is interesting that the efficacies of the peptides in the BRET assay were similar their

relative ability to block SDF-1 promoted inhibition of adenylyl cyclase activity (Fig. 6D). Indeed, whereas TMs II and IV acted as complete inhibitors in both assays, TMs VI and VII acted as partial blockers at 10 μM. When considering the inverse-agonist TC14012, only TMII significantly attenuated the ligand-
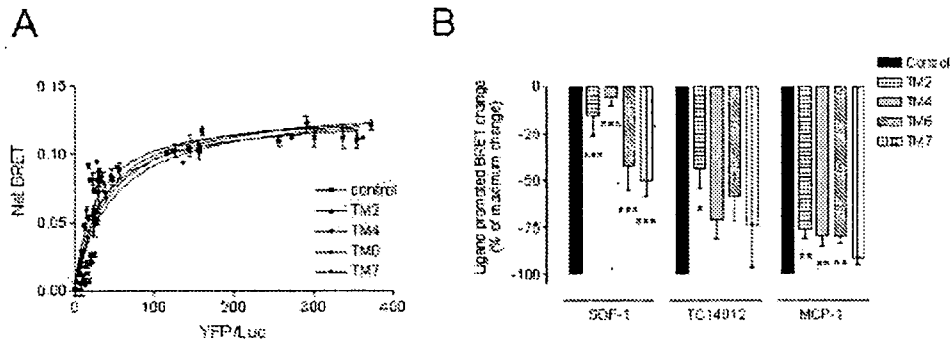
A B

FIG. 7. **Effects of CXCR4 TM peptides on CCR2-CXCR4 heterodimers.** *A*, saturation curve of CCR2-CXCR4 heterodimers in the presence and absence of CXCR4 TM peptides. HEK293T cells transfected with 0.1 μg of CCR2-Luc and increasing quantities of CXCR4-YFP were incubated for 15 min at 37 °C in presence or absence of 10 μM of CXCR4 TMII, TMIV, TMVI, or TMVII before BRET measurement. *B*, HEK293T cells transfected with 0.1 μg of CCR2-RLuc and a saturating excess (1.0 μg) of CXCR4-YFP were treated with 10 μM of each CXCR4 TM peptide and stimulated with either 200 nM SDF-1, 100 nM TC14012, or 200 nM MCP-1. Results are expressed as the mean ± S.E. of five independent experiments carried out in triplicate. Asterisks indicate statistical significance of the difference between the TM-treated condition and control condition (vehicle alone, *black bar*) with ***, $p < 0.001$; **, $p < 0.01$; *, $p < 0.05$. Absence of asterisk indicates $p > 0.05$.

promoted BRET reduction; TMs IV, VI, and VII led only to marginal inhibition that did not reach statistical significance (Fig. 6B). The inhibitory action of the peptides seems to be directly linked to the inhibition of the activation process and not to the ligand binding to the receptor, because neither SDF-1 nor TC14012 binding to CXCR4 was affected by the peptides (data not shown). The differential effect of the peptides on the agonist- and inverse agonist-promoted changes further confirmed that the two ligands promoted distinct conformational changes that are differentially affected by the peptides. The effect was specific for CXCR4 because the peptides did not interfere with the MCP-1-induced increase of the CCR2 homodimer BRET signal (Fig. 6C). In addition, two peptides derived from the β2-adrenergic receptor TM VI (38) were without effect on the SDF-1 promoted increase in BRET between CXCR4-RLuc and CXCR4-YFP (data not shown).

We then examined the effect of the CXCR4-derived peptides on the CXCR4/CCR2 heterodimer. In the absence of ligands, the four peptides had no effect on the basal heterodimer BRET signal obtained between CCR2-RLuc and CXCR4-YFP (Fig. 7A), similar to what was observed for the CXCR4 homodimer. However, all four peptides blocked, albeit to different extents, the SDF-1-promoted BRET change, although only TMII significantly affected the TC14012-induced BRET reduction (Fig. 7B). This pattern of inhibition, which is similar to that observed for the CXCR4 homodimer suggests that comparable CXCR4 conformational changes occur upon ligand binding whether the receptor is part of an homodimer or within a CXCR4/CCR2 heterodimer. It is interesting that a modest (~25%) but statistically significant reduction of the heterodimer BRET response to the CCR2-selective agonist MCP-1 was also observed upon treatment with the CXCR4-derived TMII, TMIV, and TMVI peptides (Fig. 7B). This observation suggests that the heterodimer conformational changes induced by ligand binding to a single receptor protomer may not only involve changes within the ligand-bound receptor. Instead, trans-receptor conformational reorganization may be transmitted to the CXCR4 protomer upon ligand binding to the CCR2 protomer, and these transmitted conformational changes could be blocked by the CXCR4-derived peptides. On the other hand, the observed effects may be related to the capacity of the CXCR4-bound peptides to reduce CCR2 movements within the heterodimer.

DISCUSSION

Recent appreciation that GPCRs exist as dimers has raised a number of questions regarding the molecular dynamics and functional role of such oligomeric organization. Among these, whether dimerization is a constitutive phenomenon or is promoted by ligand binding remains highly debated. The role of dimerization in the receptor activation process also remains poorly understood. In this article, we present evidence indicating that, at least for CXCR4 and CCR2, receptors exist as constitutive homo- and heterodimers and that ligand binding induces conformational changes within pre-existing complexes without promoting the formation or dissociation of dimers. Taking advantage of CXCR4-derived peptides that can non-competitively block receptor function, we also showed that ligand promoted changes in dimer conformations are intimately linked with receptor function.

Previous studies have led to conflicting interpretations concerning the dynamic nature of GPCR dimers. In particular, although many authors interpreted ligand-promoted changes in resonance energy transfer signals between GPCR protomers as evidence for receptor dimer formation or dissociation, (9, 12–14, 48), others inferred conformational changes within constitutive receptor dimers (16, 17, 41).

When considering CXCR4 and CCR2, early co-immunoprecipitation studies suggested that dimers formed only after stimulation with chemokines (20–22). Later work using either fluorescence or bioluminescence resonance energy transfer methods revealed the existence of spontaneous CXCR4 dimers (3, 4, 24). In two of these studies, the effect of the agonist SDF-1- was assessed on the basal RET signals. Whereas a modest increase that did not reach statistical significance was observed in one study (4), a reproducible increase was observed in the other (24). However, the data obtained did not allow determination of whether the RET augmentation represented an increase in dimer formation or a conformational change within the preformed dimers.

In the present study, in addition to confirming the existence of constitutive CXCR4 homodimers, our BRET results demonstrate that both CCR2 homodimers and CXCR4/CCR2 heterodimers can form spontaneously. Three lines of evidence supported that the basal BRET signals observed truly represent specific constitutive dimerization and are not simply non-specific "bystander BRET" that would result from tight random-packing of monomeric receptors: 1) BRET titration experiments gave rise to saturating hyperbolic curves that are characteristic of specific protein-protein interactions rather than random molecular collisions (39), 2) no specific BRET signal could be detected between either CXCR4 or CCR2 and the unrelated GABAbR2, 3) receptor occupancy resulted in

BRET Reveals Ligand-induced Conformational Change

either ligand-specific increases or decreases of the BRET signal; such a result would not be expected if the basal BRET signal resulted from nonspecific random collisions. In addition, the receptor expression levels of the transfected cells used in this study are similar to those observed in primary lymphocytes, thereby excluding the idea that dimerization is a result of receptor overexpression.

Our study also provides a conclusive demonstration that ligand-promoted modulation of CXCR4 and CCR2 homo- and heterodimer BRET signals results not from changes in dimer numbers but from the rearrangements of preformed dimers. First, the BRET titration curves revealed that the BRET$_{50}$ values, which would be expected to change if the propensity to form dimers was affected (39, 49), were unaltered in the presence of an agonist or an inverse agonist, suggesting that the ligands did not affect the apparent affinity of the receptor protomers for one another. Changes in maximal BRET signal in the absence of apparent altered affinity is best explained by conformational changes that change the distance and/or orientation between the energy donor and acceptor affecting the energy transfer efficacy. Second, the dependence of the MCP-1-promoted change in BRET signal on the orientation of the CXCR4/CCR2 heterodimer BRET partners (*i.e.* MCP-1 increased the BRET signal for the CXCR4-RLuc/CCR2-YFP pair but decreased it for CCR2-RLuc/CXCR4-YFP) is hardly compatible with ligand-promoted dimer formation or dissociation. In fact, it seems highly unlikely that the fluorophore fusion orientation alone would determine whether MCP-1 induces dimer association or dissociation. Rather, the dependence of the BRET changes (*i.e.* increase or decrease) on the BRET pair configuration probably reflects structural particularities of the respective pairs studied. Indeed, the specific initial structural state determined by the particular combination of a receptor C terminus fused to either the energy donor or the acceptor could greatly influence how the same conformational switch is sensed by the BRET partners.

Considering the extent of the BRET changes promoted by various ligands for the CXCR4 homodimer, our results seem to contradict the previously reported CXCR4 model proposed by Trent *et al.* (50). In this model, the inverse agonist T140 is predicted to induce only minor rearrangements, whereas more important changes are expected from the binding of the weak agonist AMD3100. It should be pointed out, however, that the model only considered the monomeric form of the receptor; it is perhaps more important that the initial state was assimilated to a fully inactive conformation (based on the available rhodopsin structure (51)). Taking into account the previous report that CXCR4 displays a level of spontaneous activity that can be inhibited by TC14012 but is almost not affected by AMD3100 in cells (42), one could propose that the average basal dimer conformation detected by BRET represents a partially activated conformation that resembles the one stabilized by AMD3100. It follows that AMD3100 would not promote important conformational changes thus only marginally affecting the basal BRET signal, whereas the stabilization of a fully inactive conformation by TC1402 would be translated in considerable BRET changes, which is what we observed in living cells.

In the case of the CXCR4 and CCR2 homodimers, ligand-induced changes in BRET signals nicely parallel the intrinsic efficacy of the ligands; that is, agonists promote signal increases (a full agonist yielding a greater response than a partial agonist) whereas inverse agonists decrease the signal. It would therefore be tempting to speculate that the direction of the BRET changes reflects specific conformational changes that can be directly linked to the signaling efficacy. However,

the data obtained with the CXCR4/CCR2 heterodimer questions such a direct relationship. Indeed, the CCR2 agonist MCP-1 either increased or decreased the BRET signal depending on the BRET partner orientation used (see above), demonstrating that the direction of ligand-induced BRET signal inflection may depend on C-terminal structural constraints and thus differ in different systems. It would thus be prudent to conclude that different BRET changes reflect distinct ligand-stabilized receptor conformations but cannot be used to predict intrinsic efficacies. Similar conclusions have already been suggested by other authors (16).

Although no direct relationship between the direction of the BRET changes induced by ligands and their intrinsic efficacies can be strictly established, our data with the CXCR4-derived TM peptides strongly suggest that the conformational changes detected are linked to receptor activity. The original underlying rationale for testing the effect of the inhibitory peptides developed by Tarasova *et al.* (36) was that TM-derived peptides could bind to the protomer interface within dimers, thereby interfering with dimerization and inhibiting receptor activities. Indeed, the activity of a similar peptide has been suggested to result from the disruption of the $\beta2$-adrenergic receptor dimers (38), an interpretation that is in line with the proposed roles of TM domains in other GPCR dimer interfaces (52, 53). Hernanz-Falcon *et al.* recently reported that simultaneous mutation of two residues located in the first and fourth TM domains abolished CCR5 dimerization, and that small peptides corresponding to these regions had the same effect (48). On the other hand, it has been proposed that TM-peptides can act by interfering with intramolecular TM packing, thus inducing receptor distortion (54). Our finding that CXCR4 TM-derived peptides did not affect basal BRET levels indicate that they did not function by inhibiting dimerization or by causing major distortion in the initial conformation, because both of these should have caused detectable BRET changes. Our data suggest rather that peptide binding stabilizes the initial conformation hampering the occurrence of any ligand-promoted conformational changes. Given the anti-HIV activity of these peptides (Ref. 36 and data not shown), this interpretation has important implications for the role of CXCR4 in HIV entry, in that it suggests that the peptides could block envelope-induced conformational changes of CXCR4 that are mandatory for viral entry. It remains to be investigated whether the apparently different efficacy of the various peptides to inhibit both function and ligand-promoted conformational changes reflects the respective importance of specific TM domains in the dimerization process.

The observation that CXCR4-derived TM peptides could block the conformational rearrangement of the CXCR4/CCR2 heterodimer promoted by the selective CCR2 agonist MCP-1 provides some clues about the functional organization of chemokine receptor dimers. Indeed, these results demonstrate that the presence of only one selective chemokine is sufficient to change the conformation of the heterodimer. In addition, it is tempting to speculate that conformational changes could be transmitted *in trans* from one protomer to the other. Such interprotomer transmission of conformational changes would suggest that the activity of one receptor could be affected by ligand binding to the other. This type of transactivation has been shown previously for the metabotropic GABAb receptor, where agonist binding to the GABABR1 protomer led to the functional engagement of the heterotrimeric G protein by the GABAbR2 protomer (55, 56). The occurrence of trans-dimer conformational rearrangements could have great impact on the therapeutic use of receptor ligands because they may impinge

not only on the activity of the cognate receptor but also on that of the heterodimer partner. On the other hand, however, our results could also be explained by the capacity of the CXCR4-derived peptides to interfere with CCR2 movements within the heterodimer.

The fact that CXCR4/CCR2 heterodimers are conformationally responsive to selective ligands of either receptor could have potentially important physiological implications. Cell migration frequently involves several chemokines, and the mechanisms leading to the integration of these multiple signals are poorly understood (57–59). Because many chemokine receptors are co-expressed in the same cell types and can be involved together in a single migration process, a role for heterodimers in integrating the multiple signals could be envisioned. For example, CCR2 and CXCR4 have been shown to both contribute to accumulation of activated/memory T-cells in lymph node (60). Whether they play sequential roles or are simultaneously activated, possibly by the intermediate of receptor heterodimers, will require further investigations.

REFERENCES

1. Terrillon, S., and Bouvier, M. (2004) *EMBO Rep.* 5, 30–34
2. McVey, M., Ramsay, D., Kellett, E., Rees, S., Wilson, S., Pope, A. J., and Milligan, G. (2001) *J. Biol. Chem.* 276, 14092–14099
3. Issafras, H., Angers, S., Bulenger, S., Blanpain, C., Parmentier, M., Labbe-Jullie, C., Bouvier, M., and Marullo, S. (2002) *J. Biol. Chem.* 277, 34666–34673
4. Babcock, G. J., Farzan, M., and Sodroski, J. (2003) *J. Biol. Chem.* 278, 3378–3385
5. Terrillon, S., Durroux, T., Mouillac, B., Breit, A., Ayoub, M. A., Taulan, M., Jockers, R., Barberis, C., and Bouvier, M. (2003) *Mol. Endocrinol.* 17, 677–691
6. Canals, M., Marcellino, D., Fanelli, F., Ciruela, F., de Benedetti, P., Goldberg, S. R., Neve, K., Fuxe, K., Agnati, L. F., Woods, A. S., Ferre, S., Lluis, C., Bouvier, M., and Franco, R. (2003) *J. Biol. Chem.* 278, 46741–46749
7. Gazi, L., Lopez-Gimenez, J. F., Rudiger, M. P., and Strange, P. G. (2003) *Eur. J. Biochem.* 270, 3928–3938
8. Dinger, M. C., Bader, J. E., Kobor, A. D., Kretzschmar, A. K., and Beck-Sickinger, A. G. (2003) *J. Biol. Chem.* 278, 10562–10571
9. Kroeger, K. M., Hanyaloglu, A. C., Seeber, R. M., Miles, L. E., and Eidne, K. A. (2001) *J. Biol. Chem.* 276, 12736–12743
10. Cornea, A., Janovick, J. A., Maya-Nunez, G., and Conn, P. M. (2001) *J. Biol. Chem.* 276, 2153–2158
11. Wurch, T., Matsumoto, A., and Pauwels, P. J. (2001) *FEBS Lett.* 507, 109–113
12. Berglund, M. M., Schober, D. A., Esterman, M. A., and Gehlert, D. R. (2003) *J. Pharmacol. Exp. Ther.* 307, 1120–1126
13. Grant, M., Collier, B., and Kumar, U. (2004) *J. Biol. Chem.* 279, 36179–36183
14. Cheng, Z. J., and Miller, L. J. (2001) *J. Biol. Chem.* 276, 48040–48047
15. Latif, R., Graves, P., and Davies, T. F. (2002) *J. Biol. Chem.* 277, 45059–45067
16. Ayoub, M. A., Couturier, C., Lucas-Meunier, E., Angers, S., Fossier, P., Bouvier, M., and Jockers, R. (2002) *J. Biol. Chem.* 277, 21522–21528
17. Ayoub, M. A., Levoye, A., Delagrange, P., and Jockers, R. (2004) *Mol. Pharmacol.*
18. Tateyama, M., Abe, H., Nakata, H., Saito, O., and Kubo, Y. (2004) *Nat. Struct. Mol. Biol.* 11, 637–642
19. Rodriguez-Frade, J. M., Vila-Coro, A. J., de Ana, A. M., Albar, J. P., Martinez, A. C., and Mellado, M. (1999) *Proc. Natl. Acad. Sci. U. S. A.* 96, 3628–3633
20. Mellado, M., Rodriguez-Frade, J. M., Vila-Coro, A. J., de Ana, A. M., and Martinez, A. C. (1999) *Nature* 400, 723–724
21. Vila-Coro, A. J., Rodriguez-Frade, J. M., Martin De Ana, A., Moreno-Ortiz, M. C., Martinez, A. C., and Mellado, M. (1999) *FASEB J.* 13, 1699–1710
22. Mellado, M., Rodriguez-Frade, J. M., Vila-Coro, A. J., Fernandez, S., Martin de Ana, A., Jones, D. R., Toran, J. L., and Martinez, A. C. (2001) *EMBO J.* 20, 2497–2507
23. Rodriguez-Frade, J. M., Del Real, G., Serrano, A., Hernanz-Falcon, P., Soriano, S. F., Vila-Coro, A. J., De Ana, A. M., Lucas, P., Prieto, I., Martinez, A. C., and and Mellado, M. (2004) *EMBO J.* 23, 66–76
24. Toth, P. T., Ren, D., and Miller, R. J. (2004) *J. Pharmacol. Exp. Ther.* 310, 8–17
25. Lee, B., Doranz, B. J., Rana, S., Yi, Y., Mellado, M., Frade, J. M., Martinez, A. C., O'Brien, S. J., Dean, M., Collman, R. G., and Doms, R. W. (1998) *J. Virol.* 72, 7450–7458
26. Smith, M. W., Dean, M., Carrington, M., Winkler, C., Huttley, G. A., Lomb, D. A., Goedert, J. J., O'Brien, T. R., Jacobson, L. P., Kaslow, R., Buchbinder, S., Vittinghoff, E., Vlahov, D., Hoots, K., Hilgartner, M. W., and O'Brien, S. J. (1997) *Science* 277, 959–965
27. Tang, J., Shelton, B., Makhatadze, N. J., Zhang, Y., Schaen, M., Louie, L. G., Goedert, J. J., Seaberg, E. C., Margolick, J. B., Mellors, J., and Kaslow, R. A. (2002) *J. Virol.* 76, 662–672
28. Feng, Y., Broder, C. C., Kennedy, P. E., and Berger, E. A. (1996) *Science* 272, 872–877
29. Murphy, P. M. (2001) *N. Engl. J. Med.* 345, 833–835
30. Nanki, T., Hayashida, K., El-Gabalawy, H. S., Suson, S., Shi, K., Girschick, H. J., Yavuz, S., and Lipsky, P. E. (2000) *J. Immunol.* 165, 6590–6598
31. Lukacs, N. W., Berlin, A., Schols, D., Skerlj, R. T., and Bridger, G. J. (2002) *Am. J. Pathol.* 160, 1353–1360
32. Salcedo, R., and Oppenheim, J. J. (2003) *Microcirculation* 10, 359–370
33. Lapidot, T. (2001) *Ann. N. Y. Acad. Sci.* 938, 83–95
34. Charo, I. F., and Peters, W. (2003) *Microcirculation* 10, 259–264
35. Tamamura, H., Omagari, A., Hiramatsu, K., Gotoh, K., Kanamoto, T., Xu, Y., Kodama, E., Matsuoka, M., Hattori, T., Yamamoto, N., Nakashima, H., Otaka, A., and Fujii, N. (2001) *Bioorg. Med. Chem. Lett.* 11, 1897–1902
36. Tarasova, N. I., Rice, W. G., and Michejda, C. J. (1999) *J. Biol. Chem.* 274, 34911–34915
37. Heveker, N., Tissot, M., Thuret, A., Schneider-Mergener, J., Alizon, M., Roch, M., and Marullo, S. (2001) *Mol. Pharmacol.* 59, 1418–1425
38. Hebert, T. E., Moffett, S., Morello, J. P., Loisel, T. P., Bichet, D. G., Barret, C., and Bouvier, M. (1996) *J. Biol. Chem.* 271, 16384–16392
39. Mercier, J. F., Salahpour, A., Angers, S., Breit, A., and Bouvier, M. (2002) *J. Biol. Chem.* 277, 44925–44931
40. Brelot, A., Heveker, N., Montes, M., and Alizon, M. (2000) *J. Biol. Chem.* 275, 23736–23744
41. Couturier, C., and Jockers, R. (2003) *J. Biol. Chem.* 278, 26604–26611
42. Zhang, W. B., Navenot, J. M., Haribabu, B., Tamamura, H., Hiramatu, K., Omagari, A., Pei, G., Manfredi, J. P., Fujii, N., Broach, J. R., and Peiper, S. C. (2002) *J. Biol. Chem.* 277, 24515–24521
43. Gupta, S. K., Pillarisetti, K., Thomas, R. A., and Aiyar, N. (2001) *Immunol. Lett.* 78, 29–34
44. Hesselgesser, J., Liang, M., Hoxie, J., Greenberg, M., Brass, L. F., Orsini, M. J., Taub, D., and Horuk, R. (1998) *J. Immunol.* 160, 877–883
45. Haribabu, B., Richardson, R. M., Fisher, I., Sozzani, S., Peiper, S. C., Horuk, R., Ali, H., and Snyderman, R. (1997) *J. Biol. Chem.* 272, 28726–28731
46. Di Salvo, J., Koch, G. E., Johnson, K. E., Blake, A. D., Daugherty, B. L., DeMartino, J. A., Sirotina-Meisher, A., Liu, Y., Springer, M. S., Cascieri, M. A., and Sullivan, K. A. (2000) *Eur. J. Pharmacol.* 409, 143–154
47. Doranz, B. J., Orsini, M. J., Turner, J. D., Hoffman, T. L., Berson, J. F., Hoxie, J. A., Peiper, S. C., Brass, L. F., and Doms, R. W. (1999) *J. Virol.* 73, 2752–2761
48. Hernanz-Falcon, P., Rodriguez-Frade, J. M., Serrano, A., Juan, D., del Sol, A., Soriano, S. F., Roncal, F., Gomez, L., Valencia, A., Martinez, A. C., and Mellado, M. (2004) *Nat. Immunol.* 5, 216–223
49. Ramsay, D., Kellett, E., McVey, M., Rees, S., and Milligan, G. (2002) *Biochem. J.* 365, 429–440
50. Trent, J. O., Wang, Z.-x., Murray, J. L., Shao, W., Tamamura, H., Fujii, N., and Peiper, S. C. (2003) *J. Biol. Chem.* 278, 47136–47144
51. Palczewski, K., Kumasaka, T., Hori, T., Behnke, C. A., Motoshima, H., Fox, B. A., Le Trong, I., Teller, D. C., Okada, T., Stenkamp, R. E., Yamamoto, M., and Miyano, M. (2000) *Science* 289, 739–745
52. Overton, M. C., and Blumer, K. J. (2002) *J. Biol. Chem.* 277, 41463–41472
53. Guo, W., Shi, L., and Javitch, J. A. (2003) *J. Biol. Chem.* 278, 4385–4388
54. George, S. R., Lee, S. P., Varghese, G., Zeman, P. R., Seeman, P., Ng, G. Y. K., and O'Dowd, B. F. (1998) *J. Biol. Chem.* 273, 30244–30248
55. Galvez, T., Duthey, B., Kniazeff, J., Blahos, J., Rovelli, G., Bettler, B., Prezeau, L., and Pin, J. P. (2001) *EMBO J.* 20, 2152–2159
56. Kniazeff, J., Galvez, T., Labesse, G., and Pin, J. P. (2002) *J. Neurosci.* 22, 7352–7361
57. Foxman, E. F., Campbell, J. J., and Butcher, E. C. (1997) *J. Cell Biol.* 139, 1349–1360
58. Foxman, E. F., Kunkel, E. J., and Butcher, E. C. (1999) *J. Cell Biol.* 147, 577–588
59. Moser, B., Wolf, M., Walz, A., and Loetscher, P. (2004) *Trends Immunol.* 25, 75–84
60. Yopp, A. C., Fu, S., Honig, S. M., Randolph, G. J., Ding, Y., Krieger, N. R., and Bromberg, J. S. (2004) *J. Immunol.* 173, 855–865